

**DESIGN AND CRASHWORTHINESS ANALYSIS OF A
LANDING GEAR STRUT FOR A UAV**

A Final Year Project Report

Presented to

SCHOOL OF MECHANICAL & MANUFACTURING ENGINEERING

Department of Mechanical Engineering

NUST

ISLAMABAD, PAKISTAN

In Partial Fulfillment

of the Requirements of the Degree of
Bachelors of Mechanical Engineering

by

Abdul Wasay Ikhtlaq

Muhammad Uzair Malik

Syed Adil Hasan Naqvi

May 2019

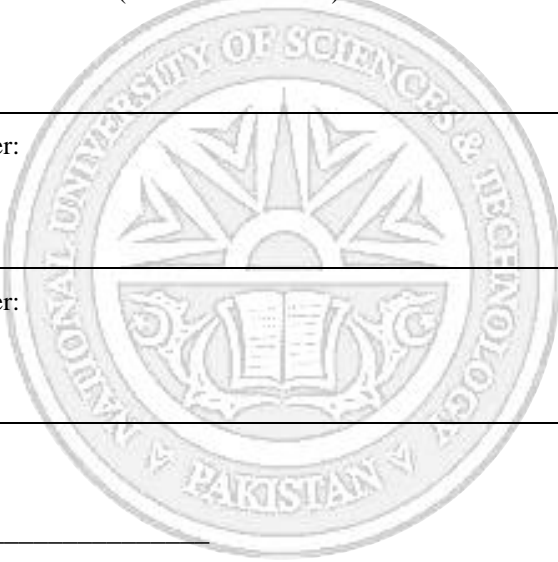
EXAMINATION COMMITTEE

We hereby recommend that the final year project report prepared under our supervision by:

ABDUL WASAY IKHLAQ	00000127286
MUHAMMAD UZAIR MALIK	00000121451
SYED ADIL HASAN NAQVI	00000124165

Titled: “DESIGN AND CRASHWORTHINESS ANALYSIS OF A LANDING GEAR STRUT OF A UAV” be accepted in partial fulfillment of the requirements for the award of Mechanical Engineering degree with grade ____

Supervisor: Dr. Jawad Aslam (Assistant Professor)	_____ Dated:
Committee Member:	_____ Dated:
Committee Member:	_____ Dated:



(Head of Department)

(Date)

COUNTERSIGNED

Dated: _____

(Dean / Principal)

ABSTRACT

Unmanned Armed Vehicles (UAVs) are used in surveillance, offensive, and other tactical operations by the military of several countries of the world including Pakistan. The landing gear system of these UAVs has to be robust enough to bear severe loading conditions not only during normal operational conditions but also in case of any unexpected crash-landing. Of all the different components that make a landing gear system (including braking system, steering system, suspension), the most crucial is the strut as it directly handles the load of the UAV and bears the impact upon landing.

The load bearing ability of a landing gear strut can be increased by improving its design (length/overall shape/cross-sectional shape) and the material (metal/composites) it is made of. Figuring out these design parameters is an iterative process that goes back and forth between making some design changes (adding or removing material/changing shape) and analyzing the effect of said changes on the loadbearing ability of the strut using analysis tools such as ANSYS and SimuLink. This iterative process is initialized by choosing a suitable landing gear system of a UAV (Predator MQ1 in our case).

Along with this, a suitable tire is also selected based on the loading conditions. All the design parameters are tweaked keeping in mind the integration of the designed parts with other assemblies.

ACKNOWLEDGEMENTS

We would like to acknowledge the efforts of Dr. Jawad Aslam (SMME, NUST) for supervising this project and helping us through this endeavor. Dr. Aslam has provided constant support so far in this project and has helped us with any problem that we faced and with any query that we had to the best of his abilities.

We would also like to acknowledge the guidance provided to us by Engr. Naveed Ahmad (NESCOM). Mr. Ahmad was assigned to us by NESCOM and has helped us clear all ambiguities we initially had regarding the scope and deliverables of this project. He has been of great assistance till now.

FYP Final Report

ORIGINALITY REPORT

10%	3%	0%	10%
SIMILARITY INDEX	INTERNET SOURCES	PUBLICATIONS	STUDENT PAPERS

PRIMARY SOURCES

1	Submitted to M S Ramaiah University of Applied Sciences Student Paper	2%
2	Submitted to University of Hertfordshire Student Paper	1%
3	documents.mx Internet Source	1%
4	iaeme.com Internet Source	1%
5	Submitted to University of Huddersfield Student Paper	1%
6	Submitted to Universiti Teknologi Malaysia Student Paper	1%
7	Submitted to Coventry University Student Paper	1%
8	Submitted to University of Liverpool Student Paper	<1%
9	Submitted to University of New South Wales	

<1%

10

Submitted to Emirates Aviation College,
Aerospace & Academic Studies

Student Paper

<1%

11

Submitted to Central Queensland University

Student Paper

<1%

12

Submitted to Limerick Institute of Technology

Student Paper

<1%

13

Submitted to Birla Institute of Technology

Student Paper

<1%

14

Submitted to Staffordshire University

Student Paper

<1%

15

Submitted to University of Greenwich

Student Paper

<1%

16

www.irjet.net

Internet Source

<1%

17

Submitted to Oxford Brookes University

Student Paper

<1%

18

Submitted to Bolton Institute of Higher
Education

Student Paper

<1%

19

Submitted to Sim University

Student Paper

<1%

20

www.gpo.gov

Internet Source

<1%

21

Submitted to Cranfield University

Student Paper

<1%

22

Submitted to Louisiana Tech University

Student Paper

<1%

23

Submitted to Kingston University

Student Paper

<1%

24

repository.bilkent.edu.tr

Internet Source

<1%

Exclude quotes On

Exclude matches Off

Exclude bibliography On

TABLE OF CONTENTS

ABSTRACT	2
ACKNOWLEDGEMENTS	3
LIST OF TABLES	9
ABBREVIATIONS	12
NOMENCLATURE	12
CHAPTER 1: INTRODUCTION	14
Motivation:	14
Problem Statement:	14
Objectives:	14
CHAPTER 2: LITERATURE REVIEW	15
Introduction:	15
A Brief History:	15
Difference between a Shock and a Strut:	15
Types of Struts:	16
Operation:	17
Materials Used:	18
Components of a Landing Gear:	18
Recent Advancements:	18
Predator UAV:	19
Landing Gear Design for UAV:	19
UAV Landing Gear Configurations:	19
Predator landing gear strut:	22
CHAPTER 3: METHODOLOGY	22
Load Dataset:	32
Tire Selection:	33
Mathematical Modeling:	34
Stroke Calculation:	35
Compression Ratios:	35
Pressure Calculations:	36
Force Analysis:	37
Governing Equation:	37
CHAPTER 4: RESULTS AND DISCUSSIONS	39
Prototype Manufacturing:	47
Material:	47

Components:.....	47
Aluminum Prototype:	47
Material:	47
Components:.....	48
Retraction System Mechanism and Assembly Integration:	50
Comparing Results of Static and Dynamic Analysis on Simulink with Experimental Results:	51
Experimental Testing:.....	51
Simulink Results for Static Testing:	54
Comparison:.....	56
Dynamic Testing Observations and Calculations:	57
Simulink Results for Dynamic Testing:.....	61
Comparison:.....	64
CHAPTER 5: CONCLUSION	68
REFERENCES	70

LIST OF TABLES

Table 1: Tail Wheel Type Advantages & Disadvantages	20
Table 2: Tandem Type Advantages vs. Disadvantages	21
Table 3: Tricycle Type Advantages vs. Disadvantages	21
Table 4: DH Parameters	50
Table 5: Testing Results Comparison	51
Table 6: Static Testing Observations and Calculations	53
Table 7: Force vs. Stiffness	54
Table 8: Forces corresponding to Mass	57

LIST OF FIGURES

Figure 1: A shock & a strut	15
Figure 2: An oleo strut	17
Figure 3: Tail wheel configuration.....	20
Figure 4: Tandem type configuration.....	20
Figure 5: Tricycle configuration.....	21
Figure 6: MQ9 Main landing gear strut.....	22
Figure 7: Approach Phase 1	23
Figure 8: Approach Phase 2	25
Figure 9: Upper cylinder model	26
Figure 10: Lower cylinder model.....	26
Figure 11: Torque links	27
Figure 12: Wheel assembly	27
Figure 13: Landing gear assembly	28
Figure 14: Simulink Settings.....	28
Figure 15: Simulink Model	29
Figure 16: Analysis parameters.....	30
Figure 17: Simulink Model	31
Figure 18: The forcing function	31
Figure 19: Standard aircraft geometry.....	32
Figure 20 - Tire sizing tables.....	34
Figure 21: Positions, velocity, accelerations vs time	39
Figure 22: Velocity vs. time	40
Figure 23 - Acceleration vs. time	41
Figure 24: Velocity vs. time	41
Figure 25: Acceleration vs. time.....	42

Figure 26: Stresses on toque link under compression	43
Figure 27: Deformations in lower cylinder	43
Figure 28: Stresses in lower cylinder	44
Figure 29: Torque link deformation	44
Figure 30: Wheel stresses.....	44
Figure 31: Wheel deformations.....	45
Figure 32: Upper cylinder deformations	45
Figure 33: Upper cylinder stresses	46
Figure 34: Gear assembly stresses.....	46
Figure 35: Gear assembly stresses.....	46
Figure 36: Gear Assembly Deformations.....	47
Figure 37: Retraction assembly	49
Figure 38: Frame assignment	50
Figure 39: Dynamic Testing.....	52
Figure 40: Dynamic Testing.....	52
Figure 41: Measuring pressure under load	53
Figure 42: Pressure vs. Displacement (Experimental Testing)	53
Figure 43: Force vs. Displacement (Experimental Testing).....	54
Figure 44: Simulink model.....	55
Figure 45: Distance vs. time.....	55
Figure 46: Forces vs. displacements.....	56
Figure 47: Forces vs. displacements.....	57
Figure 48: Displacement vs. time (F=44.32N).....	58
Figure 49: Displacement vs. time (F=53.16N).....	59
Figure 50 : Displacement vs. time (F=63.02N).....	59
Figure 51: Displacement vs. time (F=70.88N).....	60

Figure 52: Displacement vs. time (F=79.74N).....	60
Figure 53: Displacement vs. time (F=44.32N).....	61
Figure 54: Displacement vs. time.....	62
Figure 55: Displacement vs. time.....	62
Figure 56: Displacement vs. time.....	63
Figure 57: Displacement vs. time.....	63
Figure 58: Displacement vs. time (F=44.32N).....	65
Figure 59: Displacement vs. time (F=53.16N).....	65
Figure 60: Displacement vs. time (F=62.02N).....	66
Figure 61 : Displacement vs. time (F=79.74N).....	66
Figure 62 : Displacement vs. time (F=70.88N).....	67

ABBREVIATIONS

UAV	unmanned armed vehicle
MTOW	maximum take-off weight
CoG	center of gravity
LCRTM	lost core resin transfer molding

NOMENCLATURE

H	vertical height of the UAV
a	retardation
b	distance from nose to main wheel
N_f	fwd CoG from nose wheel
N_a	aft CoG from the nose wheel
A	tire selection constant
B	tire selection constant
W_w	weight of the wheel
μ_{fric}	frictional coefficient

\dot{X}	rate of stroke compression
F_{air}	frictional force of air
W	weight of the aircraft
V	sink speed
g	gravitational acceleration
L	wing lift
S	stroke
S_t	tire deflection
μ_{hyd}	hydraulic damping coefficient
d	displaced volume

CHAPTER 1: INTRODUCTION

Motivation:

1. Interest in aviation

Aviation is quite an interesting field and not having studied any aviation related course in our degree, we were quite curious about the things this field had to offer. Two of the group members also had a chance to study aviation while participating in Design Build and Fly competition a year ago. So, our interest in this project was only natural.

2. Reducing probability of damage upon crash-landing

UAVs are almost always carrying expensive and sensitive equipment which are prone to damage given the harsh conditions UAVs are expected to operate in. Keeping this in mind, it is essential that a near-perfect landing gear system be utilized to minimize the cost of damage repairs by ensuring smooth landings.

3. Strengthen national defense by providing better quality UAVs

This project originated in NESCOM, one of the top scientific and engineering organizations in Pakistan. Any research we do during this project, any breakthrough that we make, might just end up setting a base for further development of better-quality UAVs in Pakistan strengthening our defenses.

Problem Statement:

Design and Crashworthiness Analysis of a Landing Gear Strut for a UAV

Objectives:

The objectives of this project are as following:

1. Provide a landing gear strut design
2. Increase crashworthiness of the strut
3. Select a suitable tire
4. Assembly integration

CHAPTER 2: LITERATURE REVIEW

Introduction:

A strut is a structural component used to resist longitudinal load – most commonly compression - in aircrafts and automobiles. Struts may be straight or curved based on their where they're being used.

In aircrafts, the commonly used variant is the oleo strut. A variety of aircrafts, large as well as small use an oleo strut in their landing gear. An oleo strut is a pneumatic air – oil hydraulic shock. Oleo strut is designed such that it dampens and absorbs the impact upon landing and minimizes any vertical vibrations.

It can be damaging for the structural integrity of the different components of the airplane for it to bounce upon landing. The user can lose control of the vehicle which can result in disastrous damage to life and property. A landing gear should prevent this from happening. The steel springs absorb the impact energy and transmits it to the oleo strut which makes the landing much smoother even on uneven and rough landing strips.
[2]

A Brief History:

The inspiration for struts can derive its origin from human anatomy. A strut closely resembles a bone, long, made from strong material, used to take longitudinal load. The origins of struts in architecture (mostly for bracing) can be traced back to the 19th century. However, the modern landing gear strut used in aircrafts today originated in the first half of the 20th century. Several advancements and progress have been made to the design ever since.

Difference between a Shock and a Strut:

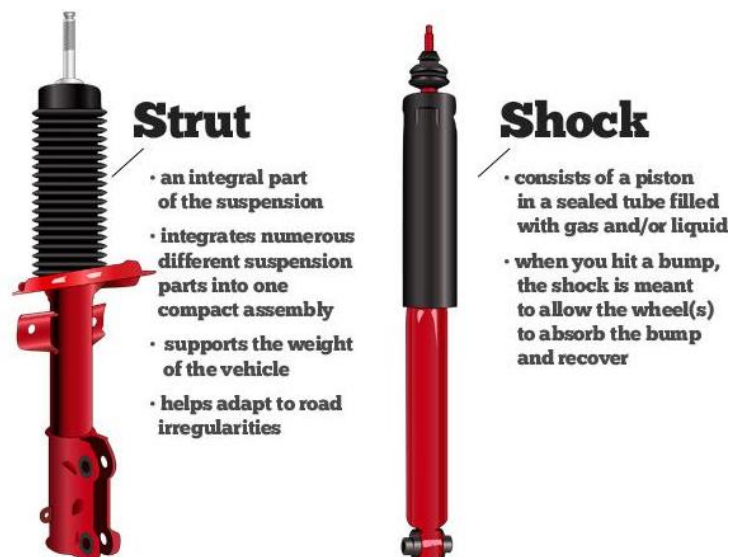


Figure 1: A shock & a strut

Although both (the shock and the strut) are similar in the job that they perform in any vehicle i.e. dampening the vibrations and the shock to minimize oscillations and ensure

smooth operation but they are very distinct in their individual characteristics. Neither can replace the other. One vehicle can either be designed to have a shock or a strut but not both at the same time. Using a shock and a strut in the same vehicle can lead to both not working correctly that defeats the purpose of their installation.

The one distinction that sets apart a shock and a strut is that in a vehicle's suspension system, a strut plays a crucial role whereas a shock does not. A strut has the ability to adjust the caster & camber angles on itself. The steering of the vehicle is dependent on the strut which also effects the angles of alignment. A strut also provides a pivot for steering. A coil spring is also contained in the strut. And because of the presence of this spring, you need alignment to replace a strut. This is also the reason that struts are typically more expensive than shocks.^[3]

Types of Struts:

Struts come in a variety of types depending on where they're being used. However, struts used in aircraft landing gear can be categorized into the following

1. Rigid struts

These are the most basic form of a landing gear. It simply consists of a rigid piece of metal (or any other material) that connects the wheels to the frame. The rigid piece is usually welded to the frame of the vehicle. However, one problem with this is that upon landing the strong shock is transmitted directly to the vehicle body. This makes the aircraft components, passengers prone to damage.

Aircraft engineers soon discovered the way to soften the landing and decrease the transfer of the impact to the body by using inflatable tires. Although this wasn't a perfect solution but it helped reduce the impact. One can still find these types of struts being used in helicopters and recreational drones.

2. Steel spring struts

To absorb the shock that is generated upon the impact of the aircraft with the ground during landing, one of the most widely used strut is the steel spring strut. These springs are made up of strong materials like aluminum and steel or other suitable composites. These springs help reduce the shock transmitted to the body by absorbing it and re-releasing it.

Upon touch-down, the spring compresses absorbing the impact. Then right after it dissipates and transfers the impact load to the body of the aircraft at such a rate that it doesn't damage the plane. These struts are generally simple, lightweight and are very easy to maintain.

3. Bungee cords

These are the most unique type of struts. This type of struts is generally used in tailwheel aircrafts and additionally in backcountry airplanes. These are as simple as they sound. They comprise of a series of elastic cords, generally wrapped in the airframe. These allow the shock of the impact to be transmitted to the aircraft body at such a rate that doesn't affect the aircraft. These can be used in a donut configuration but most are used individually to better dissipate the shock.

4. Shock struts

This type of strut can be categorized as the only one that is a truly a shock absorber. These are also called oleo or air/oil struts. They consist of a combination of nitrogen and a hydraulic fluid. These fluids help absorb and dissipate the impact shock during landing. These are mostly used on large air vehicles but can also be found on smaller aircrafts.^[1]

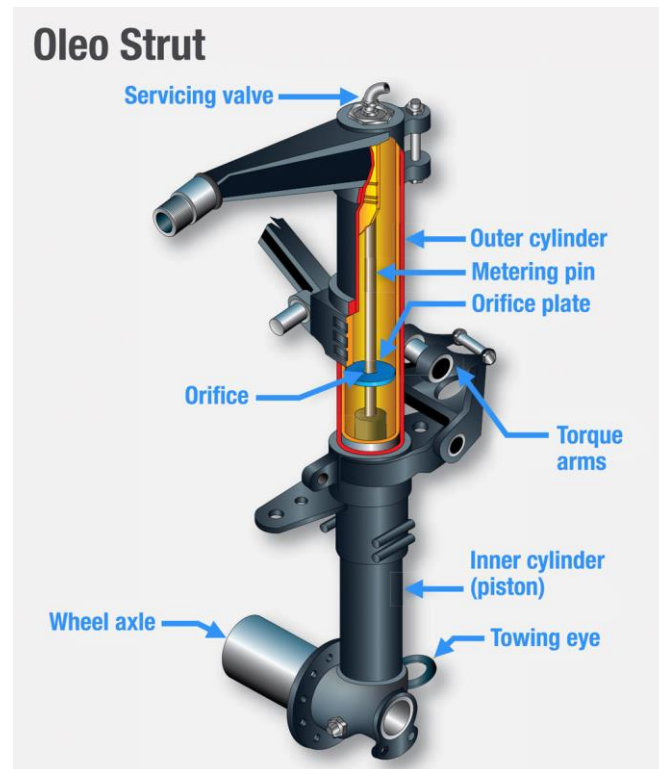


Figure 2: An oleo strut

Shock struts consist of two telescoping cylinders. The external ends of these cylinders are closed. They are attached to the body of the aircraft via the top cylinder while the bottom cylinder is attached with the landing gear. The bottom cylinder can slide freely in and out of the other one. This is also called the piston.

The bottom cylinder is almost always filled with the hydraulic fluid while nitrogen gas is contained in the upper cylinder and both of these fluids are connected via an orifice.^[1]

Operation:

There are two main jobs that struts perform.

The first one is that they provide the suspension with structural support. This is not the case in shock absorbers.

Secondly, and most importantly, a strut dampens the shock that is generated upon the impact of the aircraft with the ground. In this way, one can say that a strut is similar to a shock absorber. It consists of a piston and a piston rod. The rod is attached to the piston's end. It works against the hydraulic fluid which can control the movement of the spring as well as the suspension.

Another way a strut is similar to a shock absorber is that both are velocity sensitive. ^[5]

Materials Used:

It is important for the landing gear to be robust enough to bear the load of impact during landing. It has to be able to withstand large amounts of loads without failing. One of the most crucial in making sure a landing gear doesn't fail is the material with which the gear is constructed.

Usually steel is used being structurally strong and reliable but one of the main disadvantages of using steel is that it is too heavy and increases the overall weight of the aircraft. Titanium alloys can also be used instead of steel. Thick and heavy-duty rubber can be used to manufacture the aircraft wheels to help better absorb shocks. Other than that, many composites and elastomers can also be used.

New composites are being developed that are more structurally sound than their predecessors and have the ability to withstand large amounts of loads without failing. Cost would be one factor against the favor of such composites, which is now being overcome by improved manufacturing techniques. ^[6]

Components of a Landing Gear:

A landing gear system can be broken down into the union of many structural and system components. The structural components of a typical aircraft landing gear include:

1. Main fitting
2. Shock absorbers
3. Trailing arm
4. Axle
5. Torque links
6. Retraction actuators
7. Down-lock & up-lock mechanisms
8. Wheel & tire ^[16]

The system components are:

1. Brake unit
2. Anti-skid system
3. Extension/retraction system components

Landing gears are categorized into MLG (main landing gear) and NLG (nose landing gear). Examples of which are given in the diagrams.

Recent Advancements:

One of the most recent advances can be attributed to Improved Design of Lock - lever in an Aircraft Landing Gear for Reduction of Stress Concentration. A shear pin is a safety device inserted into a hole drilled through a driving gear (lock-lever) and two lugs in a landing gear. Its main function is to lock the driving gear in place when force is applied, and to break in the case of overload, during landing. However, considerable stress concentration can develop in the shear pin when a repeated load is applied owing to a sharp lock-lever corner that can lead to elevated local stresses where fatigue cracks

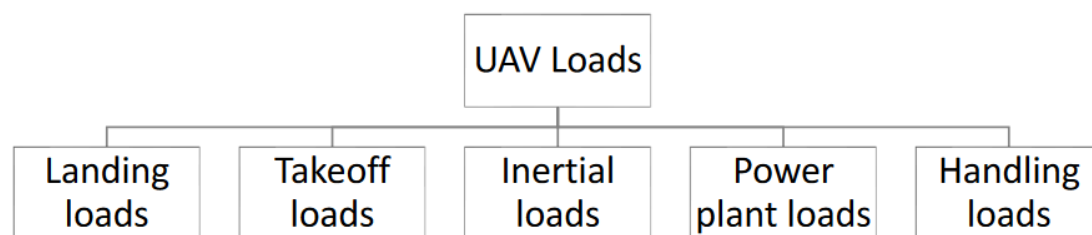
can originate. Accordingly, a specially designed corner was adopted that has a smooth surface with appropriate curvature and sharpness. The proposed design leads to a reduced stress concentration relative to the existing one. Thus, the shear pin with the presented lock-lever is relatively resistant to fatigue and damage, and easy to break when the load becomes excessive. ^[10]

Predator UAV:

One of the most commonly known unmanned aerial vehicle is the Predator. Due to its use mostly in military-based operations, it needs to be able to be air borne on demand as fast and as efficiently as possible. One of the most important aspect of a Predator's design to affect its ability to take off and land back on the safe ground is its landing gear.

The landing gear of this particular UAV is most often retractable and in tricycle configuration as shown in the figure below.

The landing gear bears several axial loads along with bending loads. A categorization of some of the loads bore by the UAV is given as following. ^[11]



Landing Gear Design for UAV:

Since the engineering design data specific to Predator UAV is not publicly available, we decided to focus our effort on the landing gear designs of the similar UAVs. So, we went through different sources including some published papers to help us study and understand the design process involved in designing a landing gear for a UAV comparable to Predator. Later we will use Predator as a benchmark for testing the performance of our designed and manufactured landing gear. ^[16]

A typical landing gear system for a UAV comprises of the following parts:

1. Strut
2. Shock Absorber
3. Extraction/Retraction Mechanism
4. Brakes
5. Wheel

UAV Landing Gear Configurations:

Landing gear system is one of the most important and crucial system for a UAV to operate normally. For a UAV to be able to stand stable on the ground or have a smooth landing, a near-perfect landing gear system is required. The landing gear helps absorb shocks that are generated upon contact with the ground during landing. The braking

system of a UAV is also integrated within the landing gear system allowing it to stop on a runway. ^[13]

We reviewed some of the landing gear configurations used in unmanned aerial vehicles along with their advantages and disadvantages. They are as following.

1. Tail wheel type

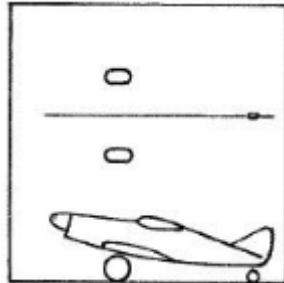


Figure 3: Tail wheel configuration

In this configuration the main landing gear is present slightly ahead of the CoG of the UAV. To prevent the UAV from tilting over, another landing gear is attached on the tail. This configuration is also named the tail-dagger gear. This kind of landing gear results in giving the angle of the fuselage as such, which allows the use of long propellers to compensate for the over-powered engines. ^[13]

Table 1: Tail Wheel Type Advantages & Disadvantages

Advantages	Disadvantages
Reduces overall weight of the UAV	Steering the UAV becomes difficult
Increases directional stability	Ground looping is also made harder as the CoG is in the latter half of the fuselage ^[13]
Damages due to rough ground is reduced	-
Overall decrease in parasitic drag	-

2. Tandem type

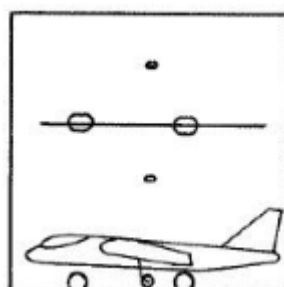


Figure 4: Tandem type configuration

In this configuration the main landing gear is aligned with the nose landing gear along the longitudinal axis of the UAV. Bicycle type arrangement is common in this configuration. Small wheels can be attached under the wings for balance. This type of landing gear allows high flexibility of wings. ^[13]

Table 2: Tandem Type Advantages vs. Disadvantages

Advantages	Disadvantages
Reduces overall weight of the UAV	Difficulty in taking-off and landing
Reduces induced drag	UAV is prone to damage while landing unevenly ^[13]
Allows UAVs to generate higher lift with low angle of attack	-

3. Tricycle type

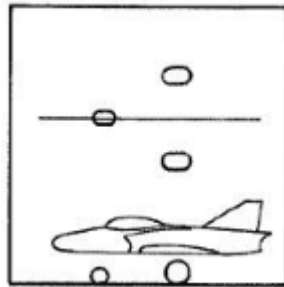


Figure 5: Tricycle configuration

This configuration resembles a tricycle. Most of the weight is supported by the main landing gear located at the latter half of the UAV ^[13]. Steering of the UAV is done by the nose landing gear located at the front of the UAV. Maneuvering can also be made easy by this configuration.

Table 3: Tricycle Type Advantages vs. Disadvantages

Advantages	Disadvantages
UAV can brake even at higher speeds without nosing over	Significant increase in drag
CoG is at optimum location preventing looping	Slight increase in UAV weight
Maneuvering is easy in this configuration	Nose gear is damage prone
UAV not effected by crosswinds	-
Weight is evenly distributed	-

Predator landing gear strut:

We were able to find the landing gear strut of Predator B MQ-9 which gave us quite some insight as to what the shape of the strut is supposed to be and what materials and techniques might be involved in its manufacturing. The most prominent primary process was lost core resin transfer molding (LCRTM). It has a hollow core which allowed the weight and material cost to be reduced while never compromising on its load bearing ability. It was 73” in length and 8” in width.^[9]



Figure 6: MQ9 Main landing gear strut

CHAPTER 3: METHODOLOGY

Approach (Phase 1):

The general approach we adopted towards our project is divided into two main sections and can be shown as

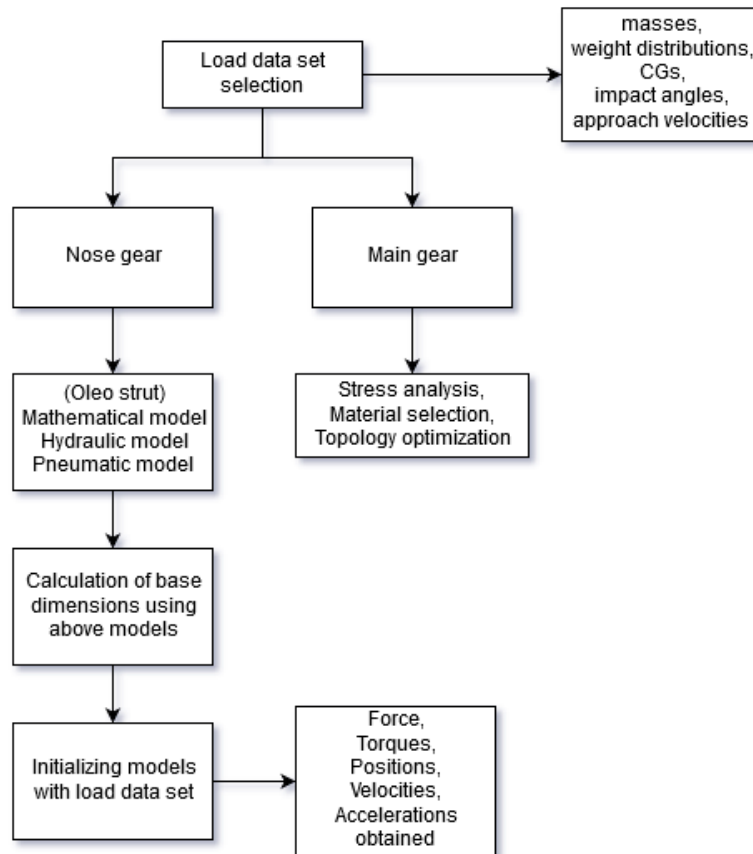


Figure 7: Approach Phase 1

Given below is a brief description of what these stages hold. These will be discussed in detail later.

Load Data Selection:

Initially we have to select a certain load data set appropriate for our conditions. This data set would constitute masses of the different parts, the weight distribution of the structure, the center of gravities. The velocity and the corresponding angle with which the airplane approaches the ground known as approach velocity and impact angle are also determined. All of this was done for a reference UAV Predator MQ-1. This was done as per the instructions of the NESCOM supervisor committee. The mentioned load data set was established for the nose gear as well as the main gear.

Main Landing Gear:

As far as the main landing gear is concerned, our task is to conduct a stress analysis (static and dynamic). From the results, we will select a material suitable for this gear. This material would of course be light in weight but strong enough to resist

deformations under the generated stresses. The last step would be topology optimization.

Nose Landing Gear:

Our main focus would be the nose landing gear. After comprehensive literature review, we started working on the mathematical modeling of the Oleo Strut. The major chunk of our project focuses on this strut and its behavior.

Mathematical Modeling:

This involves the hydraulic as well as pneumatic modeling of the oleo strut. This model completely defines the strut and its functionality. With some assumptions, almost all the characteristics of the physical model can be determined with this comprehensive mathematical model.

Calculation of Base Dimensions:

From the mathematical model constructed above, a generalized and random base dimensions set was chosen. This set is preliminary set of dimensions subjected to changes as the analysis phase goes on. A hit and trial approach is to be used to get the best possible results along with any optimization algorithms known.

Initializing Models with load data set:

When the aforementioned load data set is applied to the preliminary model, a set of forces, torques, velocities, positions and accelerations is obtained. These parameters are obtained by solving the mathematical model. Later software will also be used to get this data set.

Approach (Phase 2):

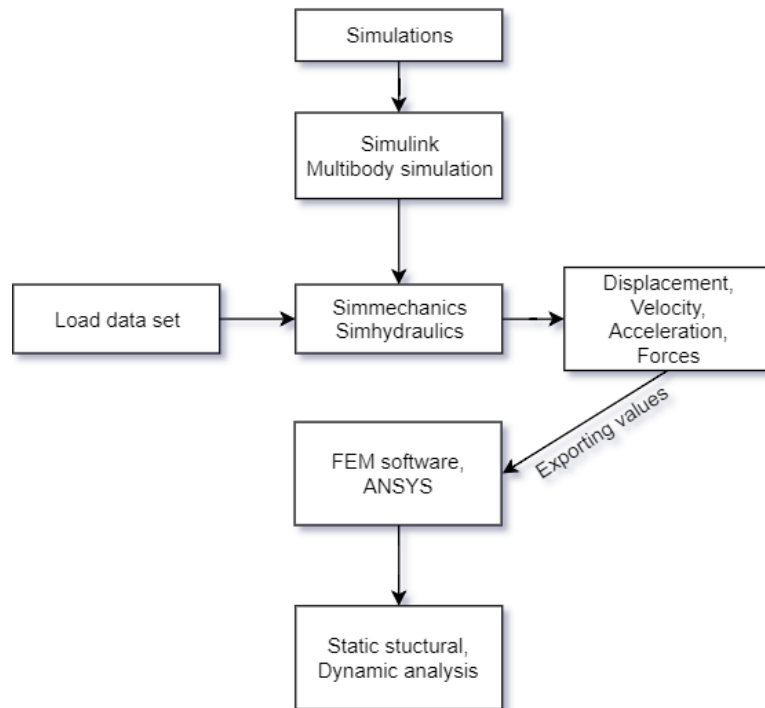


Figure 8: Approach Phase 2

Simulation:

The landing gear model was simulated on Simulink, where all the static and dynamic characteristics were modeled.

SimMechanics/SimHydraulics:

Multibody Simulation was used. SimMechanics and SimHydraulics were coupled together and excited with the given load data set to generate displacements, velocities, accelerations and forces etc. Several iterations were carried out with different base dimensions.

FEM Software:

The data set generated above is to be exported to an FEM software. We used Ansys for this purpose. Stress analysis was carried out. Static and Dynamics analyses were carried out. The spring and damping elements were set and adjusted accordingly.

Finalized Design:

After validation through several analysis techniques, a design is to be finalized. This optimal design would have the dimensions, materials and other associated parameters to completely define it.

Prototype Development:

A small-scale prototype is to be developed. The purpose of this prototype would be to realize our conceptual model into a physical one. The prototype development phase will also test our fabrication skills. This model will not help in testing the enhanced crashworthiness but it will serve the representation purpose.

CAD Model and Assembly

The landing gear consist of different parts, some of which are standard while others were modified. These parts of our specific design are mentioned below

The Upper Cylinder:

The upper cylinder of the landing gear establishes a connection between the lower assembly of the landing gear and the landing gear fixed support attached with the UAV body. It houses the fluid which performs the main function of shock absorption.

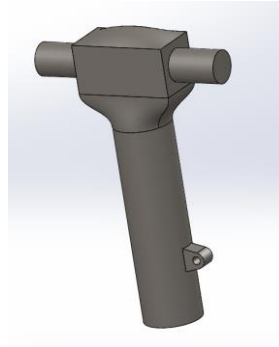


Figure 9: Upper cylinder model

The Lower Cylinder:

It acts as a piston or plunger. It compresses the fluid inside the upper cylinder when the outside force is applied. It transmits the force. It is connected to the wheel assembly through wheel axle.



Figure 10: Lower cylinder model

Torque Links:

The torque links serve to join the upper and lower cylinders. These helps distribute the torque and also change the cylindrical joint to prismatic joint. There are two torque links; the upper torque link and the lower torque link.

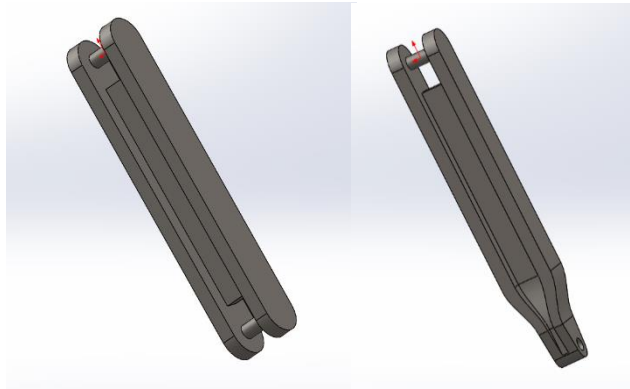


Figure 11: Torque links

Wheel Assembly:

The wheel assembly consists of the tire, the rim and the axle on which the two wheels are mounted. Currently, we made no changes in these parts and the custom parts are being used in this assembly. Although these parts will be analyzed because these play a crucial role as almost all the forces are to be transmitted through this assembly. So, the integrity of this assembly is also important.

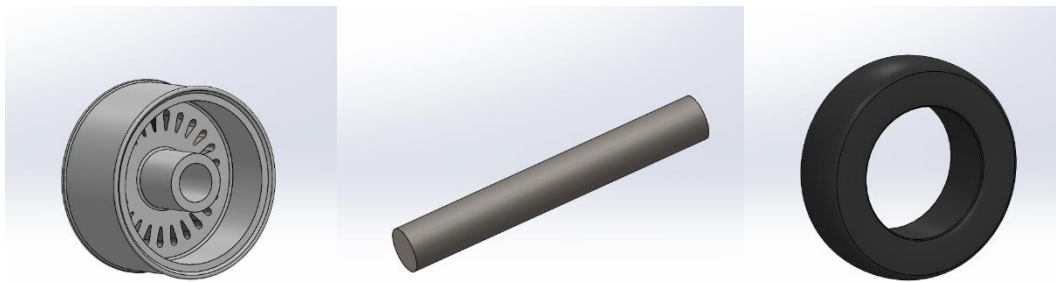


Figure 12: Wheel assembly

The Landing Gear Assembly:

The overall assembly is shown below. This is what the final design will look like. There will be changes in dimensions, properties of internal fluids and mechanisms, but the overall structure shall look the same.



Figure 13: Landing gear assembly

Modeling the Assembly in Simulink:

The CAD parts of our landing gear assembly were stored as STEP files and imported in Simulink. All the parts were imported, true to their size and physical properties. These parts were then assembled using rigid transformations and rotations. All the inertial properties of the mechanical system were kept intact.

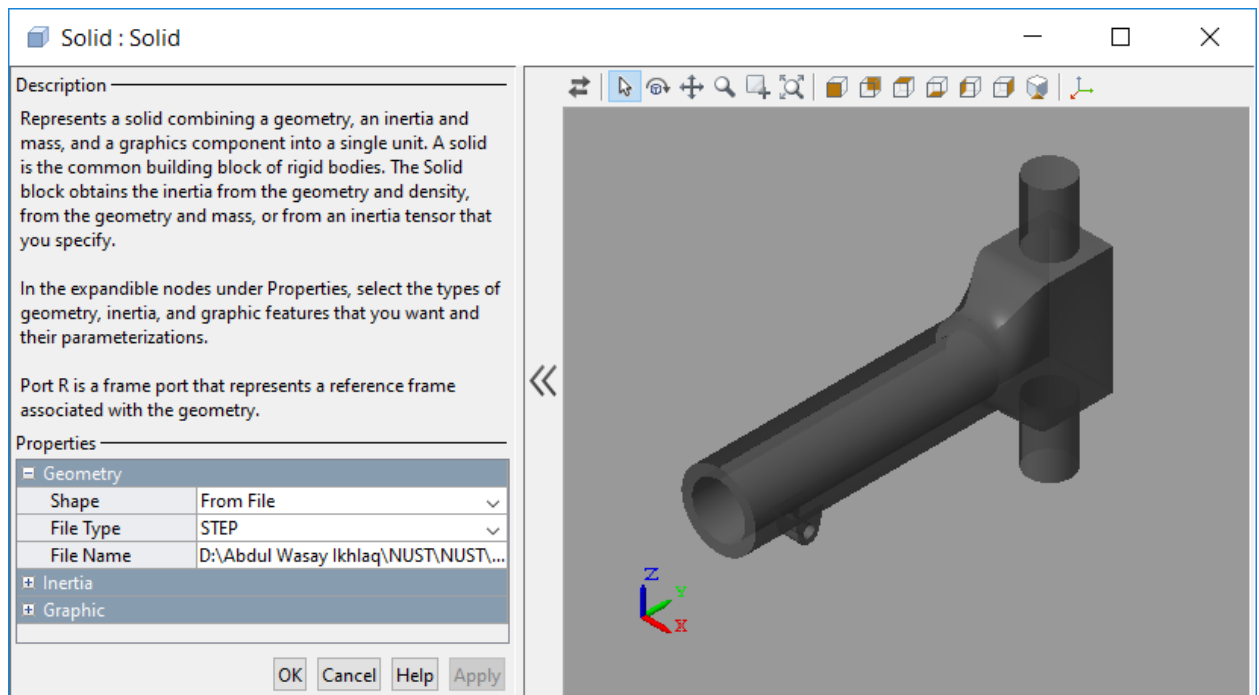


Figure 14: Simulink Settings

The unnecessary parts were neglected. These included the wheel assembly, as the wheel assembly is supposed to transmit all the force from the ground to the lower cylinder.

This is the ideal case and the case of maximum loading. At later stages, we have considered wheel assembly as well. The revolute joints were modeled accordingly.

Modeling of the Prismatic Joint/ Shock Absorbing Mechanism:

This is the most critical part of the simulation where we tried to model the shock absorbing components of the strut. From our mathematical model, we know that the oleo strut performs the shock absorption operation in 3 stages. It can be considered a combination of a spring and a damper. Hence, the prismatic joint in Simulink was modeled as a translation joint coupled to a spring of known stiffness K , and a damper of known damping c . These characteristics depend on the oil and the air ratios and volumes in the cylinder and can be varied in the modeled spring to get the best possible shock absorption. The modeled prismatic joints schematic is shown below

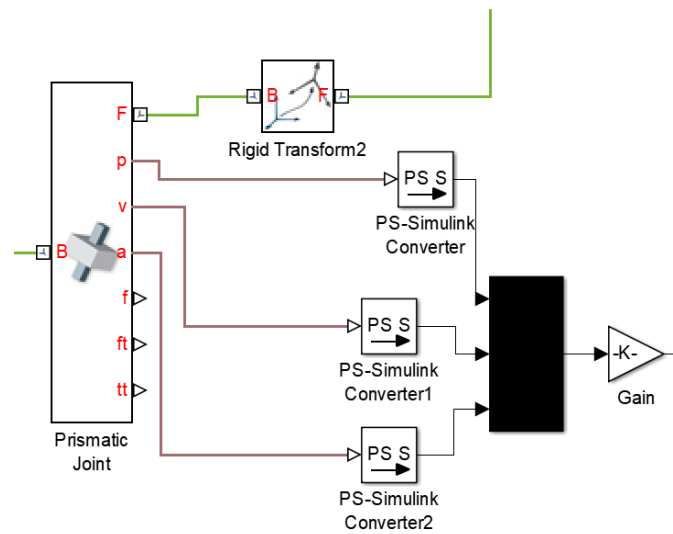


Figure 15: Simulink Model

The internal mechanics of the joint are to be varied throughout the analysis phase and one of the used samples are provided next.

Z Prismatic Primitive (Pz)		
State Targets		
Specify Position ...	<input checked="" type="checkbox"/>	
Priority	High (desired) ▾	
Value	600	mm ▾
Specify Velocity ...	<input type="checkbox"/>	
Internal Mechanics		
Equilibrium Posi...	600	mm ▾
Spring Stiffness	70000	N/m ▾
Damping Coeffi...	40	N/(m/s) ▾
Actuation		
Force	None ▾	
Motion	Automatically Computed ▾	
Sensing		
Position	<input checked="" type="checkbox"/>	
Velocity	<input checked="" type="checkbox"/>	
Acceleration	<input checked="" type="checkbox"/>	
Actuator Force	<input checked="" type="checkbox"/>	

Figure 16: Analysis parameters

An equilibrium position may also be set and varied for the system. Moreover, sensors were used with this prismatic joint to tap the values of position, velocity, acceleration etc. This joint is the main focus of the analysis. The input values are varied and the outputs are compared.

Application of a Forcing Function:

To observe the response of our system, it must first be excited by a certain forcing function. The forcing function has been obtained through interpolation from the calculated load data set. The forcing function used is a composite of several ramp functions, representing the impact of the landing gear with the ground. Initially the forcing function was kept coarse, but it was made smoother later by taking values close to each other and using values having smaller interval from the data set. The applied force increases almost linearly with time, reaches a maximum value, and then settles or dies down to the normal value of the weight of the UAV. This is the steady state of the forcing function. The schematic is shown for the forcing function.

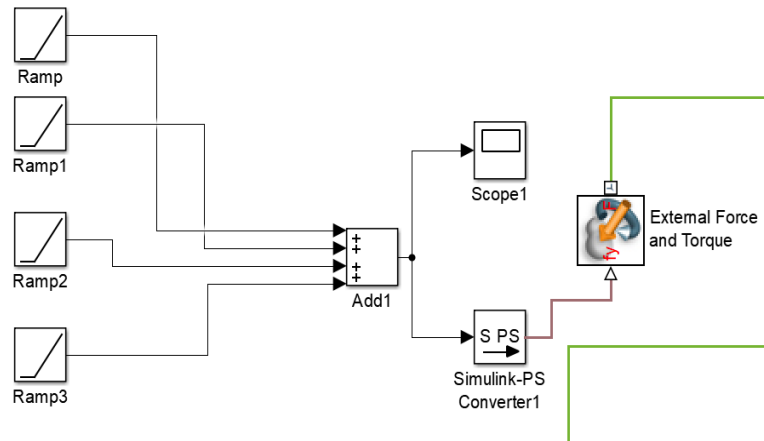


Figure 17: Simulink Model

The graphical representation of the forcing function is:

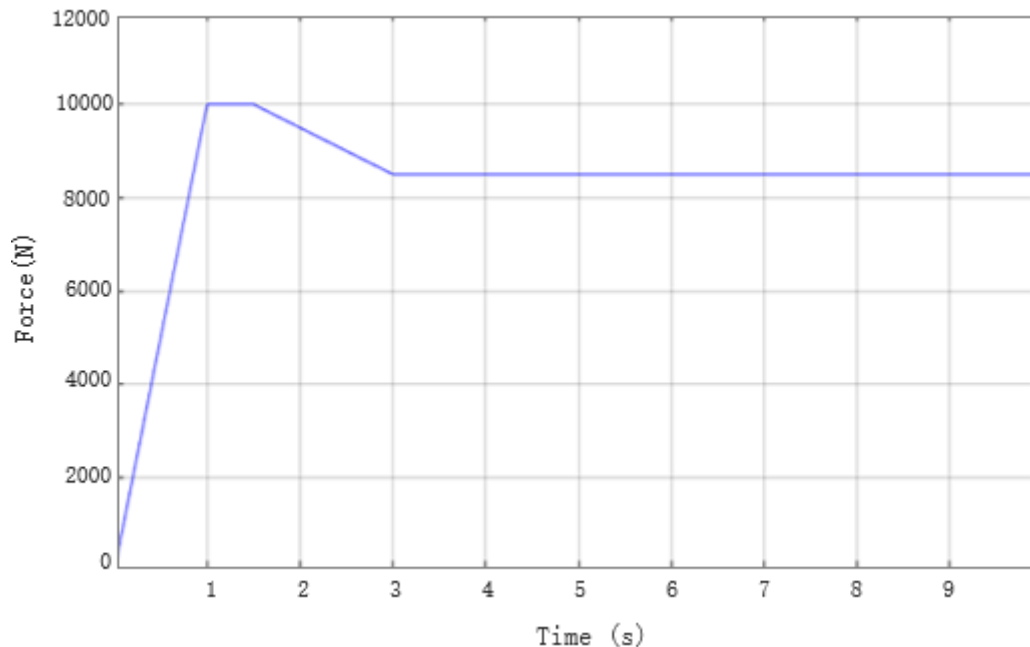


Figure 18: The forcing function

FEM Analysis:

Once the simulation is run on Simulink, we have all the necessary values of forces and torques. The assembly is imported in Ansys 18.1. the stiffness and damping properties were set. Spring element in Ansys was introduced. The static stress analysis was carried out on individual parts. A safety factor was also observed. These results validated our design to be well within the safety limits. At a later stage, we also plan to carry out dynamic analysis and crash tests. We also intend to use MSC Adams to conduct further dynamic analysis. Different materials are to be tested with the same design to make the overall design light in weight. Total deformations, directional deformations, normal stresses, shear stresses, von mises stresses are noted.

Load Dataset:

Before moving onto the design process, it is important to know what type and magnitude of loading conditions will the designed part be put through. Determining concerned loads, their magnitudes, directions can greatly help in the design process by setting upper and lower load constraints. This can be called as determining the load data set of the vehicle.

For the landing gear of an aircraft, the load data set consists of the load on the gear when the aircraft is static, when the aircraft is moving, during braking and landing.

The load data set for the UAV understudy (MQ1 Predator) is as following:

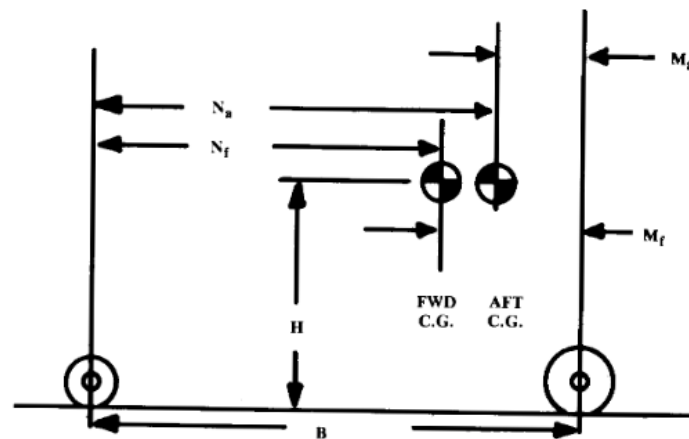


Figure 19: Standard aircraft geometry

When the UAV is standing still the total weight of the UAV is as following:

$$\text{max takeoff weight (MTOW)} = \text{predator itself} + \text{payload} + \text{fuel} \quad (1)$$

$$512 + 204 + 300 = 1020 \text{ kg} = 2250 \text{ lb}$$

Now that we have the total weight of the UAV, we can determine the total weight being applied on the main wheel and the nose wheel by using simple statics as:

$$\text{total length (nose to tail)} = 27 \text{ ft}$$

$$\text{vertical height} = H = 5 \text{ ft}$$

$$\text{retardation} = a = 10 \text{ fps}$$

$$\text{main landing gear (from nose)} = 27/2 = 13.5 \text{ ft}$$

$$\text{nose landing gear (from nose)} = 3.3 \text{ ft}$$

$$\text{nose wheel to main wheels} = B = 10.2 \text{ ft}$$

$$\text{fwd CG (from nose wheel)} = N_f = 8.5 \text{ ft}$$

$$\text{aft CG (from nose wheel)} = N_a = 9.4 \text{ ft}$$

$$\text{max static nose gear load} = F_{nose} = MTOW * \frac{B - N_f}{B} \quad (2)$$

$$= 2250 * \frac{10.2 - 8.5}{10.2} \text{ lb}$$

$$= 170 \text{ kg}$$

$$\text{max nose gear force} = 170 * \frac{9.81}{\cos(30)}$$

$$= 1926.79 \text{ N}$$

$$\text{max braking nose gear load} = MTOW * \frac{B - N_f}{B} + a * H * \frac{MTOW}{gB} \quad (3)$$

$$\text{max braking nose gear load} = 325.45 \text{ kg}$$

$$\text{max braking nose gear force} = 325.45 * \frac{9.81}{\cos(30)}$$

$$= 3686.74 \text{ N}$$

Tire Selection:

The “wheel” is the circular metal object and the rubber “tire” goes around it. It provides the necessary traction for the UAV to move on-ground and steer. Typically, the main wheel carries about 90% of the weight while the remaining 10% is carried by the nose wheel. The size of the main tire is a function on the load being applied on it as can be seen from the following equation [c]:

$$\text{diameter, width} = A * W_w^B \quad (4)$$

Once the size of the main tire is determined using the tables given below, the nose tire can easily be taken to be around 60% of the main [c].

Diameter:

$$A = 1.51$$

$$B = 0.349$$

$$D_m = 12.9 \text{ in}$$

Width:

$$A = 0.719$$

$$B = 0.312$$

$$W_m = 4.8 \text{ in} \rightarrow \text{TYPE III tire (size 5.00 - 4)}$$

Now, the nose tire can be taken to be almost 60% of the main, giving us:

$$D_m = 8 \text{ in}$$

$$W_m = 3 \text{ in}$$

Table 11.1 Statistical tire sizing

Main wheels diameter or width (in.) = $A W_W^B$	Diameter			
	Diameter		Width	
	A	B	A	B
General aviation	1.51	0.349	0.7150	0.312
Business twin	2.69	0.251	1.170	0.216
Transport/bomber	1.63	0.315	0.1043	0.480
Jet fighter/trainer	1.59	0.302	0.0980	0.467

W_W = Weight on Wheel

Table 11.2 Tire data

Size	Speed, mph	Max load, lb	Inf, psi	Max width, in.	Max diam, in.	Rolling radius	Wheel diam	Number of plies
Type III								
5.00-4	120	1,200	55	5.05	13.25	5.2	4.0	6
5.00-4	120	2,200	95	5.05	13.25	5.2	4.0	12
7.00-8	120	2,400	46	7.30	20.85	8.3	8.0	6
8.50-10	120	3,250	41	9.05	26.30	10.4	10.0	6
8.50-10	120	4,400	55	8.70	25.65	10.2	10.0	8
9.50-16	160	9,250	90	9.70	33.35	13.9	16.0	10
12.50-16	160	12,800	75	12.75	38.45	15.6	16.0	12
20.00-20	174kt	46,500	125	20.10	56.00	22.1	20.0	26
Type VII								
16 × 4.4	210	1,100	55	4.45	16.00	6.9	8.0	4
18 × 4.4	174kt	2,100	100	4.45	17.90	7.9	10.0	6
18 × 4.4	217kt	4,350	225	4.45	17.90	7.9	10.0	12
24 × 5.5	174kt	11,500	355	5.75	24.15	10.6	14.0	16
30 × 7.7	230	16,500	270	7.85	29.40	12.7	16.0	18
36 × 11	217kt	26,000	235	11.50	35.10	14.7	16.0	24
40 × 14	174kt	33,500	200	14.00	39.80	16.5	16.0	28
46 × 16	225	48,000	245	16.00	45.25	19.0	20.0	32
50 × 18	225	41,770	155	17.50	49.50	20.4	20.0	26
Three Part Name								
18 × 4.25-10	210	2,300	100	4.70	18.25	7.9	10.0	6
21 × 7.25-10	210	5,150	135	7.20	21.25	9.0	10.0	10
28 × 9.00-12	156kt	16,650	235	8.85	27.60	11.6	12.0	22
37 × 14.0-14	225	25,000	160	14.0	37.0	15.1	14.0	24
47 × 18-18	195kt	43,700	175	17.9	46.9	19.2	18.0	30
52 × 20.5-23	235	63,700	195	20.5	52.0	21.3	23.0	30

Figure 20 - Tire sizing tables

Mathematical Modeling:

To verify the results obtained by the software analysis, mathematical analysis was done.

Following parameters were calculated:

1. Stroke length
2. Compression Ratios
3. Displacement Volume
4. Pressure at different positions

5. Forces in the strut
6. Governing equation

Stroke Calculation:

The total energy of the aircraft, which is consisted of kinetic and potential energy, when it touches down, is given by:

$$E = \frac{WV^2}{2g} + (W - L)(S + S_t) \quad (5)$$

The total energy of the system can be written as:

$$\eta_s SNW + \eta_t S_t NW = \frac{WV^2}{2g} + (W - L)(S + S_t) \quad (6)$$

Value of the second value is often taken to be as 0.47 and the value of the first term is taken to be as 0. To maintain a safety an additional inch is added to the final stroke of the strut.

The first step in calculating the stroke (S) is to select the design reaction factor (N), sometimes called the landing load factor. This factor must not be mixed with the aircraft load factor, which is related to the maneuvers or atmospheric disturbances. For a transport-type or smaller aircraft and not the jet aircrafts, the landing load factor is between 0.7 and 1.5. 1.2 is the most widely used value.

After that, sink speed (V_s) is calculated. According to the rules and regulations of the FAA, the drone aircraft must withstand landing at 10 ft/s at landing weight and 6 ft/s at maximum mass of the aircraft. Practically, sink speeds of such magnitude rarely occur due to the smooth landing technology nowadays.

By knowing the drone speed, drag coefficients and other related components, wing lift L can also be easily calculated.

Compression Ratios:

We can get compression by dividing pressure in one condition by pressure in another condition. Actually, there are three positions when talking about the oleo strut which are:

1. Fully extended
2. Static
3. Fully compressed

Therefore, two compression ratios are considered which are given below:

1. From Static position to fully extended
2. From fully compressed position to static position

For mini aircraft like drone, a ratio of 2.5:1 for the static to extended case and 3:1 for the compressed to static case is taken.

Now as we know the compression ratios, if we know any one of the three pressures, we can find out the other two pressures with the help of compression ratios.

Also, by engineering statics, we can get the static force F . And with that force and piston area A , static pressure P_s is given by:

$$P_s = \frac{F}{A} \quad (7)$$

and,

$$d = SA \quad (8)$$

Pressure Calculations:

We integrate the area under the stroke and this way we find the energy that was absorbed by the strut. This relates the applied load magnitudes to stroke of the landing gear strut.

In further calculations, we'll be using 1 in the sub script to denote full extension, static position of the strut will be shown by 2 in the subscript. For compression, 3 will be used.

Generally, volume of the air that is reserved is assumed as being ten percent of the volume of total displacement d . Hence, the total air volume V_1 when the strut is at full extension is given by:

$$V_1 = V_3 + d \quad (9)$$

Moreover, as the piston of the shock absorber goes from extended to static position, this process can be defined by the isothermal compression curve.

Therefore,

$$P_1V_1 = P_xV_x = \text{constant} \quad (10)$$

Where, P_x is the pressure at any position of stroke between extended and static positions.

$$P_x = \frac{P_1V_1}{V_x} \quad (11)$$

$$P_x = \frac{P_1(V_3 + d)}{V_1 - XA} \quad (12)$$

Where, X is the position of piston anywhere between extended and static positions.

Now, as the piston of the shock absorber goes from static to fully compressed position, this process can be defined by the polytropic compression curve.

Therefore,

$$P_x = P_2 \left(\frac{V_2}{V_1 - XA} \right)^n \quad (13)$$

Where, X is the position of piston anywhere between static and fully compressed positions.

These two relations allow us to find pressure at any position during the stroke of the piston.

Force Analysis:

Holistically, the total external force acting on the shock absorber, due to impact from the ground at the time of landing, is neutralized by following three forces:

- Damping Force
- Friction – Leakage Force
- Spring Force on air

The damping force, as its name suggests, is related to the damping effect produced by the oil or fluid present in shock absorber.

It is given by:

$$F_{hyd} = \mu_{hyd} \dot{X}^2 \quad (14)$$

And,

$$\mu_{hyd} = \frac{\rho A_{piston}^3}{2(C_d A_{orifice})^2} \quad (15)$$

Friction/leakage damping force is due to the leakage of air from the gaps as well as due to the friction between the contacting surfaces.

It is given by:

$$F_{fric} = \mu_{fric} \dot{X} F_{air} \quad (16)$$

Spring force is already found out above which takes most of the impact. As calculated earlier, it is given by:

$$F_{spring} = A_{piston} P_{ext} \left(\frac{V_{ext}}{V_{ext} - A_{piston} X} \right)^n \quad (17)$$

Governing Equation:

The total force response is given by:

$$F = \frac{\dot{X}}{|\dot{X}|} \mu_{hyd} \dot{X}^2 + \mu_{fric} \dot{X} A_{piston} P_{ext} \left(\frac{V_{ext}}{V_{ext} - A_{piston} X} \right)^n + A_{piston} P_{ext} \left(\frac{V_{ext}}{V_{ext} - A_{piston} X} \right)^n \quad (18)$$

where,

1st term = Damping Force

2nd term = Friction – Leakage Force

3rd term = Spring Force on air

CHAPTER 4: RESULTS AND DISCUSSIONS

As aforementioned simulation was run in Simulink, several results were obtained. Basically, the three main parameters were noted. The prismatic joint was under consideration and its position, velocity and acceleration was noted. The parameters varied were stiffness of the spring K and the damping coefficient c . A graph formed by superimposing position, velocity and acceleration versus time is shown below for reference.

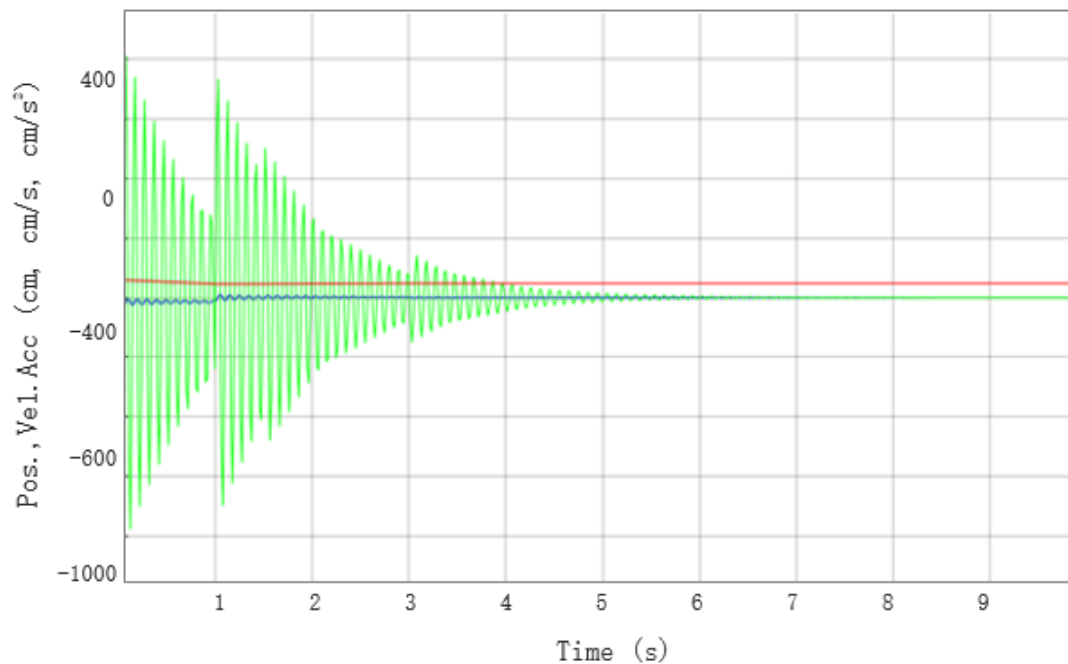


Figure 21: Positions, velocity, accelerations vs time

After several iterations, an optimal case was reached. The results for these specific values of K and c are shown below. The displacement vs time curve is shown below

The cylinder is initially at equilibrium position i.e. it is unloaded. As the cylinder impacts the ground, it moves inwards. Hence the drop in the displacement curve. The spring causes some small oscillations, which have been magnified below. Eventually, the maximum impact force acts and the displacement reaches the minimum value. After that the cylinder starts rising up and gradually settles down i.e. achieves a steady state position under the load of the UAV. This state is known as preloaded state.

The velocity vs time curve of the system is shown:

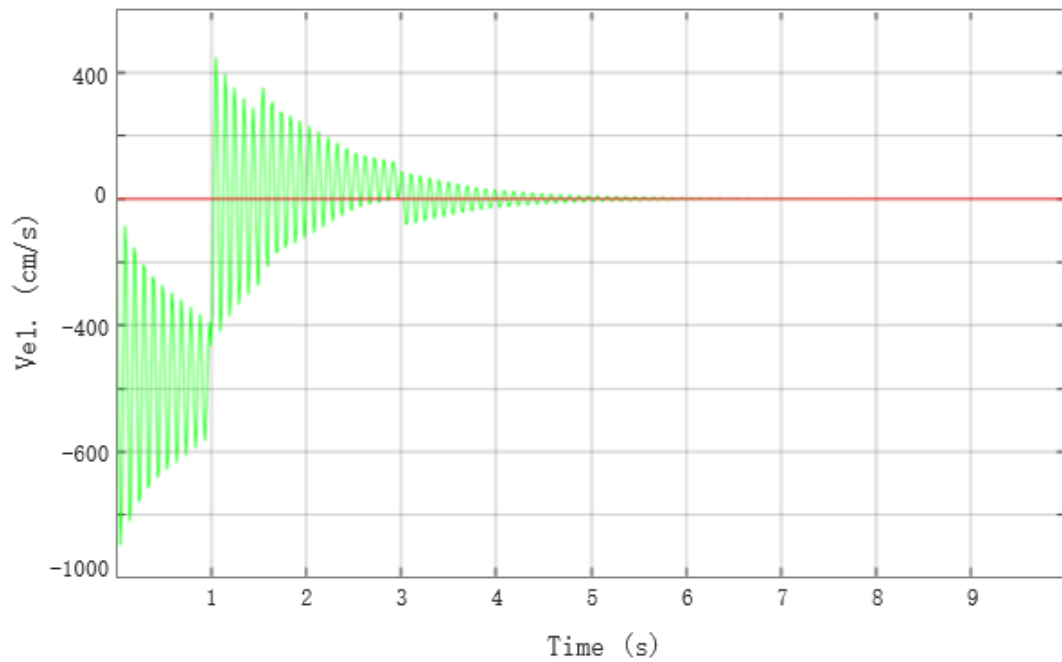


Figure 22: Velocity vs. time

The velocity trend can be explained easily. As the prismatic joint oscillates, the velocity changes directions and gradually diminishes in magnitude. At the maximum impact point, the displacement changes signs, so does the velocity. This change explains the breakpoint of the velocity curve. After the landing gear settles down, the velocity eventually reduces to zero.

The acceleration vs time curve is shown below:

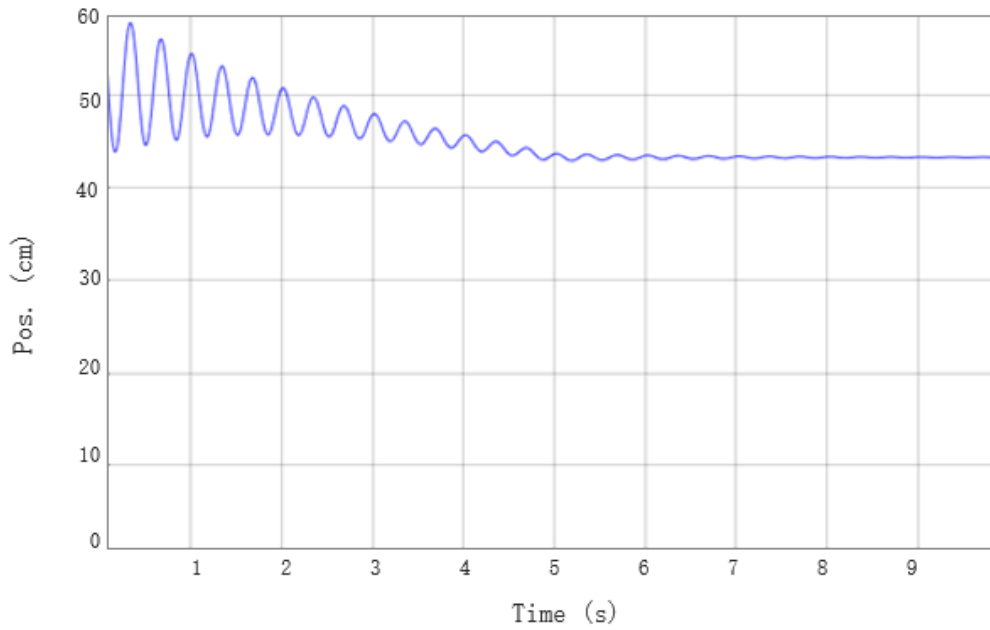


Figure 23 - Acceleration vs. time

The break point in acceleration vs time curve is the same as when the impact loading achieves maximum value. Our goal was to achieve velocity and acceleration curves with minimum maximas. Under the specific loading conditions and parameters, the maximum acceleration is 800 cm/s^2 . This is an acceptable value for our model.

Similarly, if the damping constant is reduced, the oscillations die out slowly and a delayed response is met. The results are shown below:

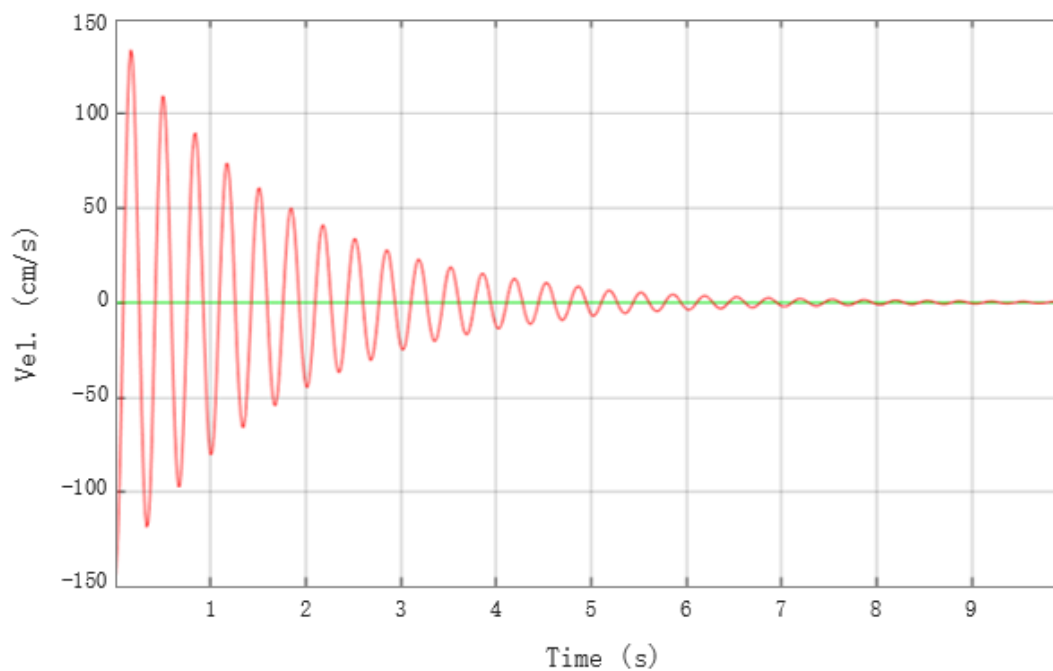


Figure 24: Velocity vs. time

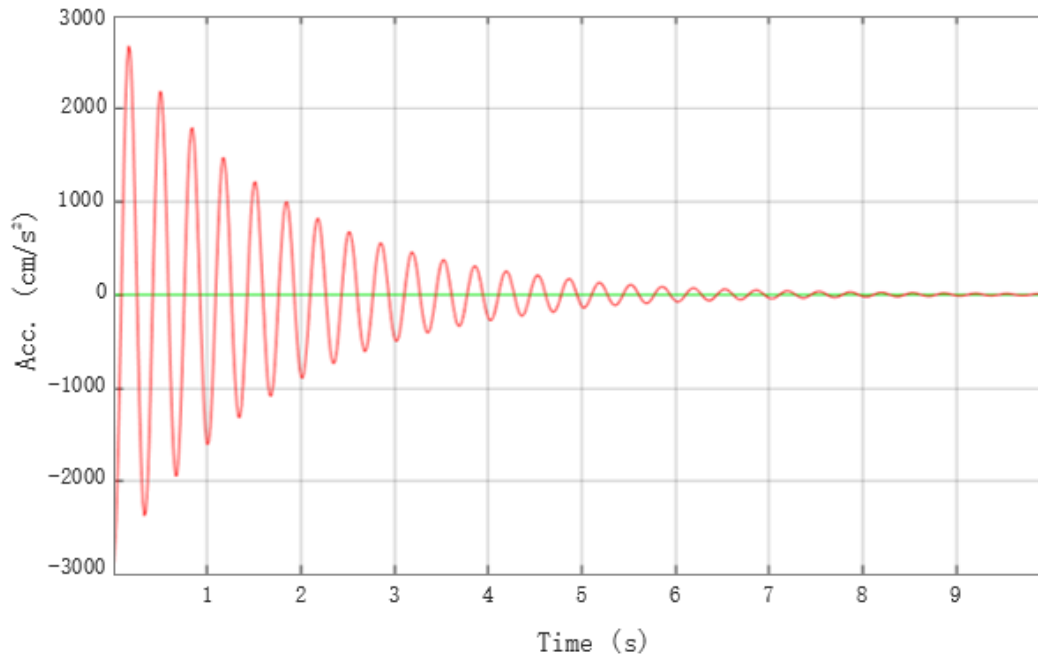


Figure 25: Acceleration vs. time

FEM Results:

The static stress analysis carried out on individual parts yielded results which have been attached below. The results were well in accordance to our expectations and guaranteed the sustainability of the materials used and the design finalized. The deformations and stresses developed in individual parts are shown next.

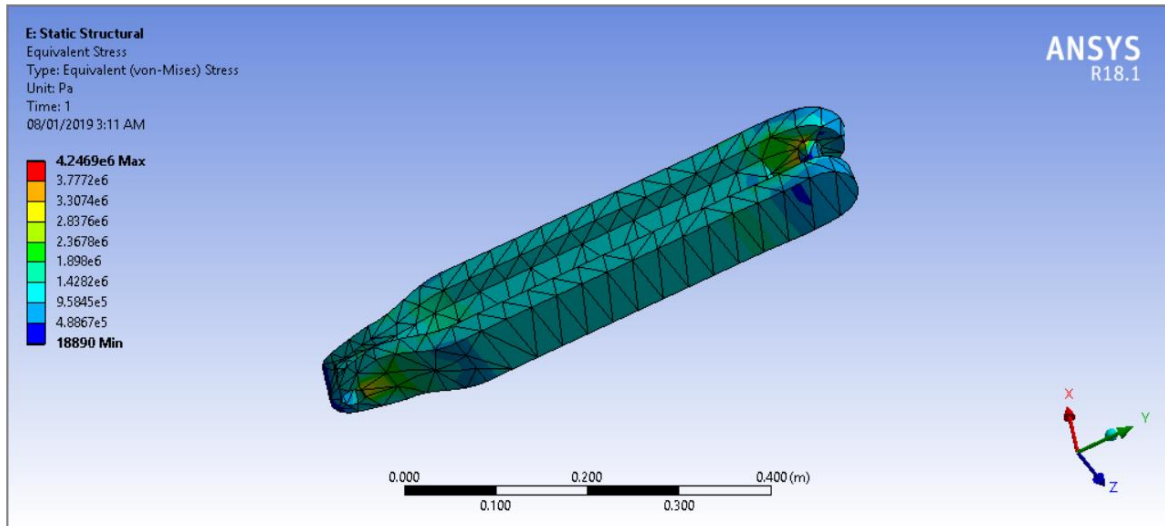


Figure 26: Stresses on torque link under compression

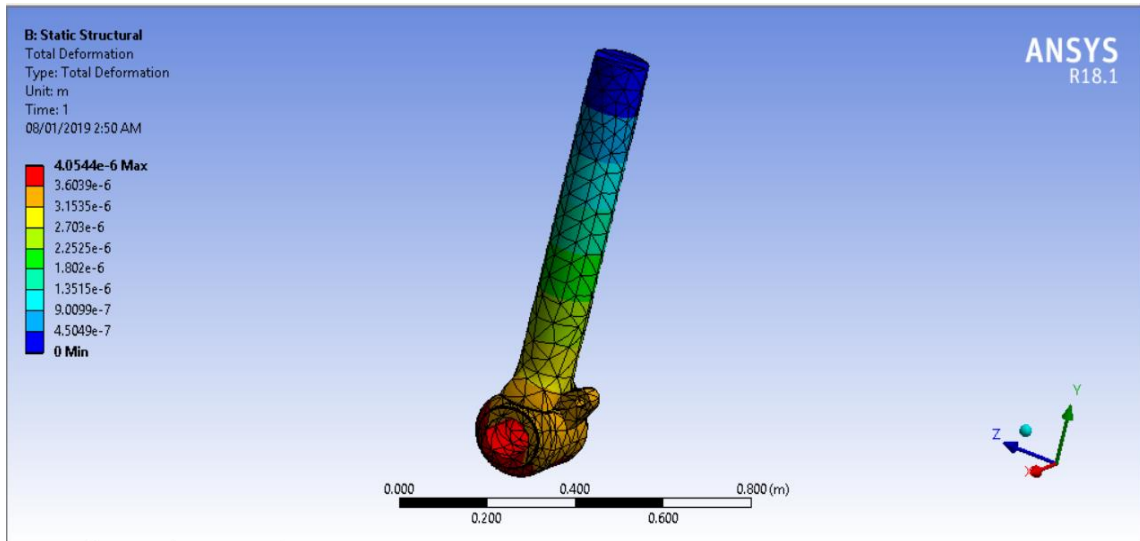


Figure 27: Deformations in lower cylinder

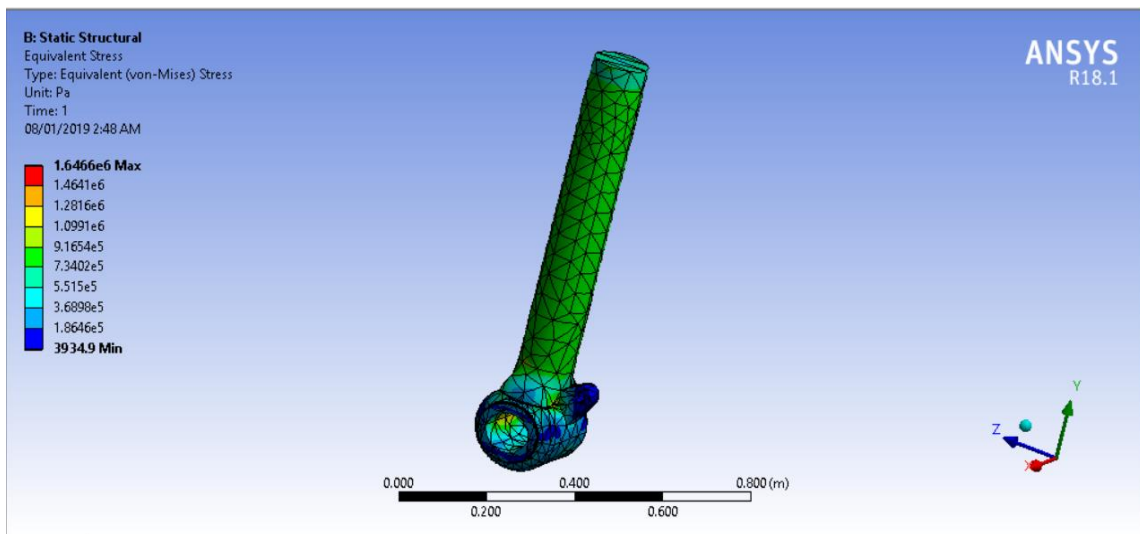


Figure 28: Stresses in lower cylinder

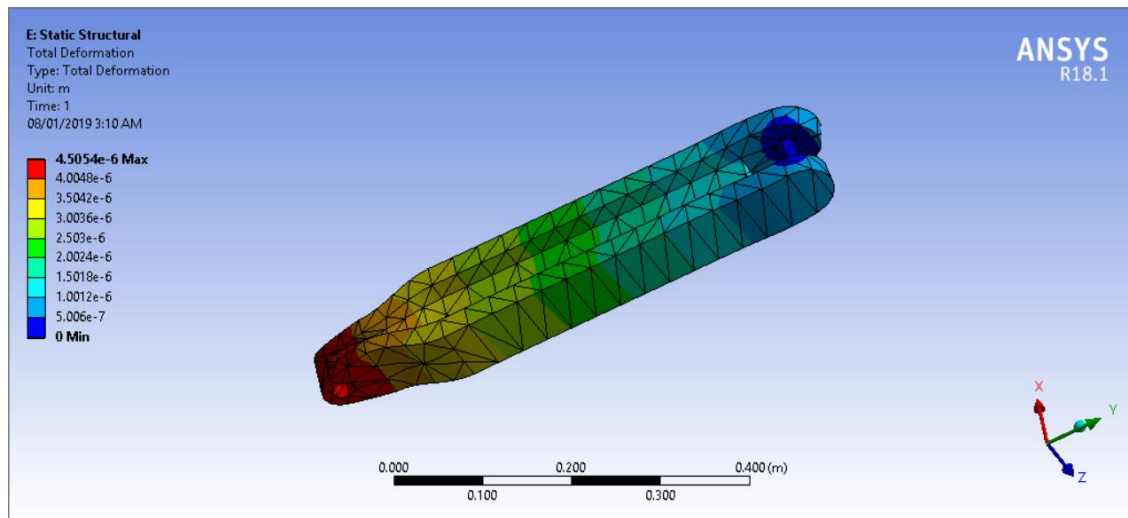


Figure 29: Torque link deformation

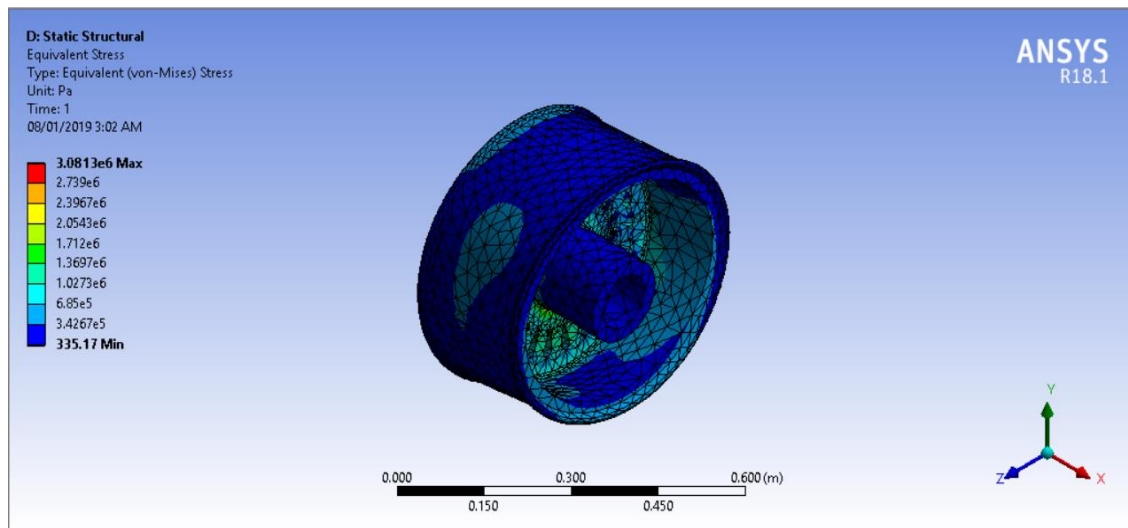


Figure 30: Wheel stresses

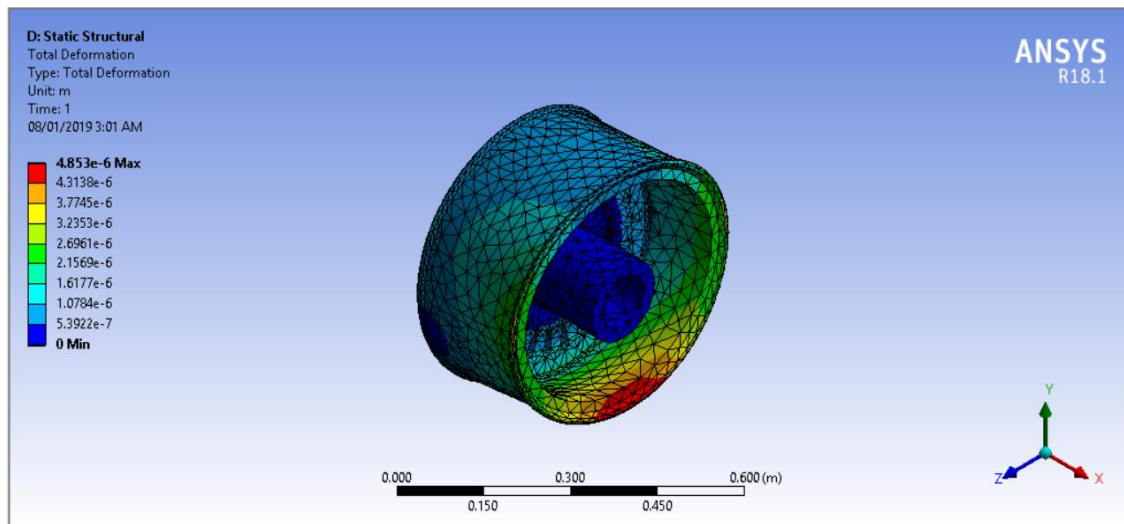


Figure 31: Wheel deformations

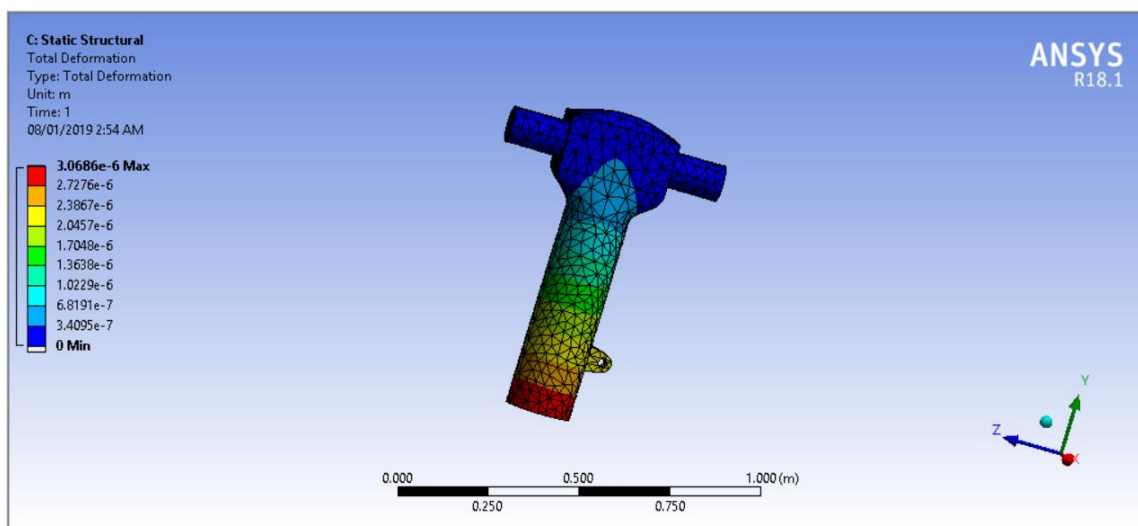


Figure 32: Upper cylinder deformations

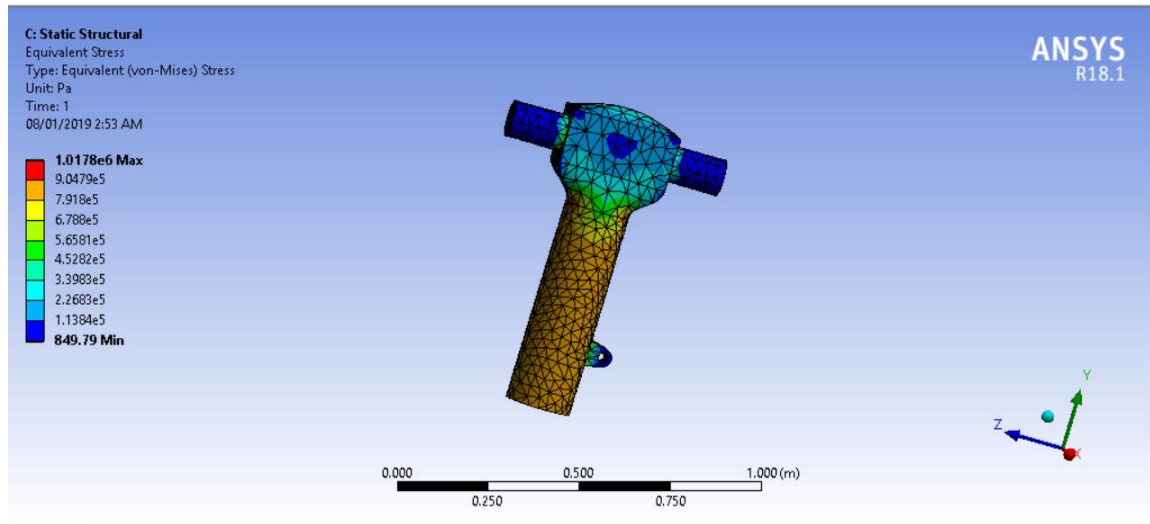


Figure 33: Upper cylinder stresses

The FEM analysis was conducted on the whole assembly to verify and validate the strength of joints and connections under the applied loadings. The spring elements were introduced as default in the ANSYS environment. The overall stress and deformation results are recorded. Other parameters such as shear stresses, normal stresses, von mises stress were also noted. The results of static structural analysis on assembly are shown:

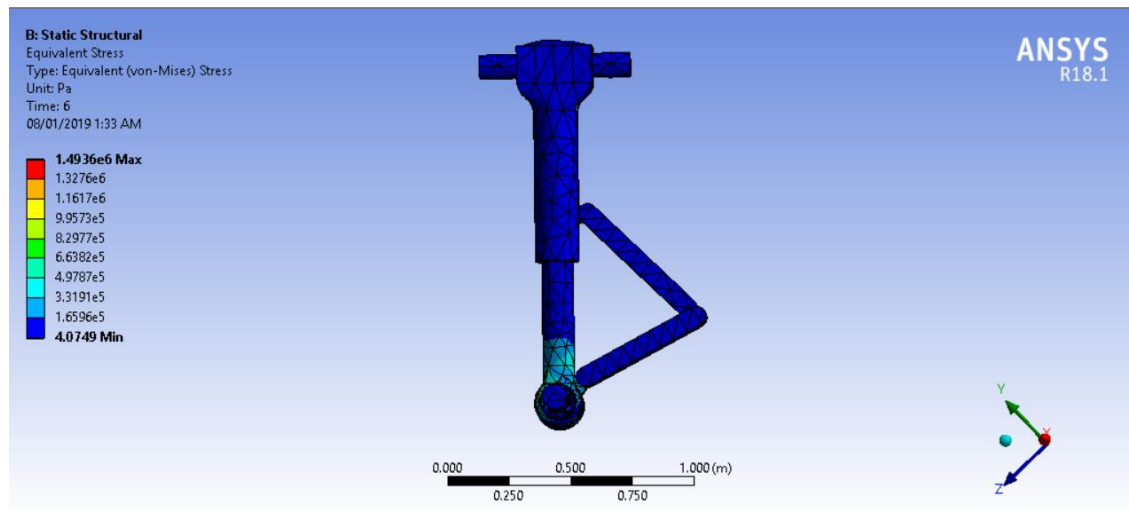


Figure 34: Gear assembly stresses

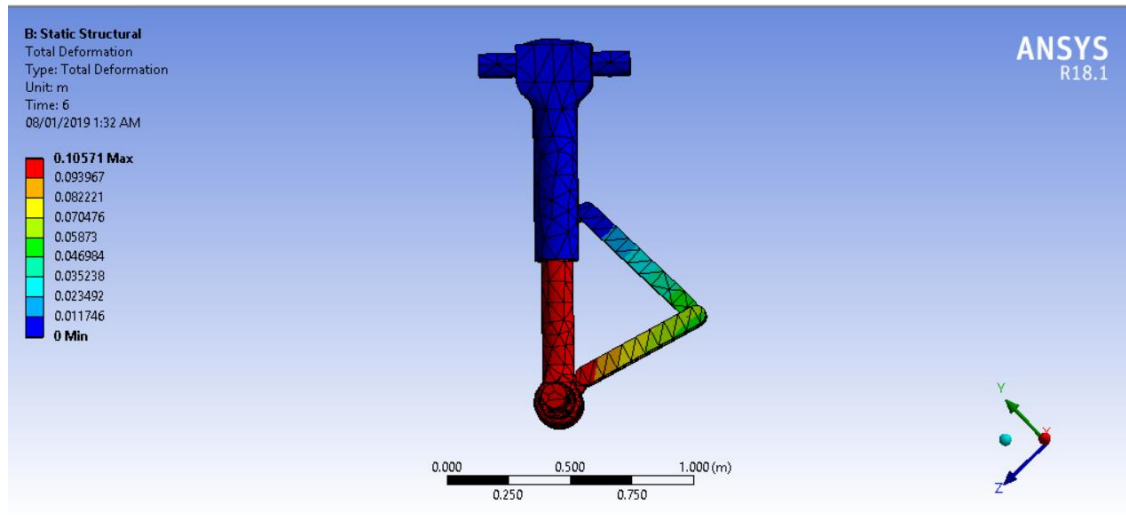


Figure 36: Gear Assembly Deformations

Prototype Manufacturing:

The dimensions were finalized according to the full-scale model. Later on, as per SMME's requirement, we had to manufacture a small-scale prototype. So the dimensions were scaled down proportionately.

Material:

We chose *perspex* as the material as it was transparent and it would allow the internal mechanism to be visible from the outside. However certain limitations were faced because of this choice of material. Due to machining limitations, the wall thicknesses were increased.

Components:

An outer cylinder was machined. It had a circular orifice plate hanging down from the top by two steel rods. The inner cylinder had a metered pin whose diameter varied along the length from the base to the top. The inner cylinder had two circular seals at the top so as to create a pressure tight environment. The assembly was filled with a hydraulic oil.

Aluminum Prototype:

Later the prototype was redesigned to fit a small RC plane that was readily available to us. The dimensioning was done again. Most of the dimensions were just scaled down from the original model. The purpose of this was to first of all test the theoretical and experimental results and then to show its integration with the RC plane assembly.

Material:

Aluminum was chosen as the main material for the strut. The orifice plate was also made up of aluminum. The steel rods were used for hanging the plate. The metering pin

was also of aluminum. Rubber seals were used. Additional hooks and clips were also made up of aluminum. Standard nuts and bolts were used for fastening purposes.

Components:

The components of the structure are the same as those used for the Perspex strut. A custom clip was made using sheet bending operations to hold the tire in place. And a rubber tire of appropriate size was pin jointed to the clip. Above the strut, an opening was made to place the pressure sensor. This sensor can be taken out of the strut if need be. Its primary purpose is to log the pressure values as the strut performs. This data can then be used for testing and record keeping purposes.

Some photos of the produced prototype are as following:



Figure 37: Metal strut



Figure 38: Strut integrated with RC plane



Figure 39: Perspex strut



Figure 37: Retraction assembly

Retraction System Mechanism and Assembly Integration:

DH Parameters for retraction assembly:

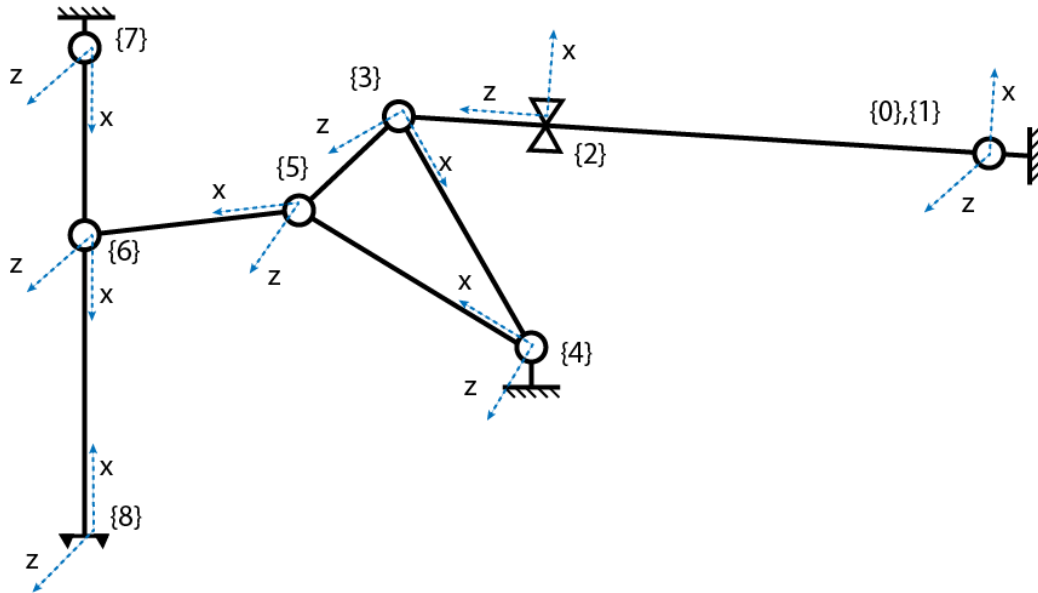


Figure 38: Frame assignment

Table 4: DH Parameters

#	a (cm)	α (deg)	d (cm)	θ (deg)
1	0	0	0	θ_1^*
2	0	-90	$L_1+L_2^*$	$\theta_2 = 0$
3	0	90	0	θ_3^*
4	$L_4 = 2.46$	0	0	$\theta_4 = 0$
5	$L_5 = 2.61$	0	0	θ_5^*
6	$L_6 = 2.52$	0	0	θ_6^*
7	$L_7 = 1.53$	0	0	$\theta_7 = 180$
8	$L_7+L_8 = 8.46$	0	0	$\theta_8 = 180$

A 6-bar retraction system was designed as discussed above. The actuator used is a linear electric actuator. At the lower extreme of the actuator position, the strut is fully retracted. While regulated arrangements were made for the length of the linear actuator at which the strut is fully extended and is at a suitable angle. Mechanical self-locking mechanism was also applied so the external retracting force would not directly affect the actuator but would be withstood by the mechanical components. The links are made up of transparent acrylic sheets as opposed to wooden sheets for their ability to resist shear stresses. These links were laser cut according to the drawings obtained from

SolidWorks. The links were pinned with the side wall of the RC plane. The actuator was controlled using Arduino UNO. The program was such that it needs to be uploaded to the microcontroller once and it would be executed indefinitely. A push button initiates the retraction or extraction process depending on the current state of the strut.

Table 5: Testing Results Comparison

Force (N)	Damping Ratio (Simulink)	Damping Ratio (Experimental)
44.32	0.7405	0.7134
53.16	0.7407	0.7256
62.02	0.7408	0.6643
70.88	0.7410	0.6148
79.74	0.7411	0.6371

Comparing Results of Static and Dynamic Analysis on Simulink with Experimental Results:

Experimental Testing:

During the experimental testing of the strut, we clamped the strut assembly vertically with pressor sensor attached. For static testing we started by placing weights on top of the strut in steps and measuring the displacement between upper and lower cylinder (compression, Δx). For the dynamic testing, we used thee second law of Newton which states that the rate of change of momentum equals the applied force. So, to simulate the dynamic conditions, objects of varying mass were dropped from a known height. The object velocities at impact point were determined mathematically and the impact time was assumed to be half a second. This assumption was made after observing several testing results and timing the impacts. Hence a linear appropriate impact force was approximated. During the momentum transfer, the appropriate coefficient of restitution for steel on steel was used. The arrangement or the setup is shown below.

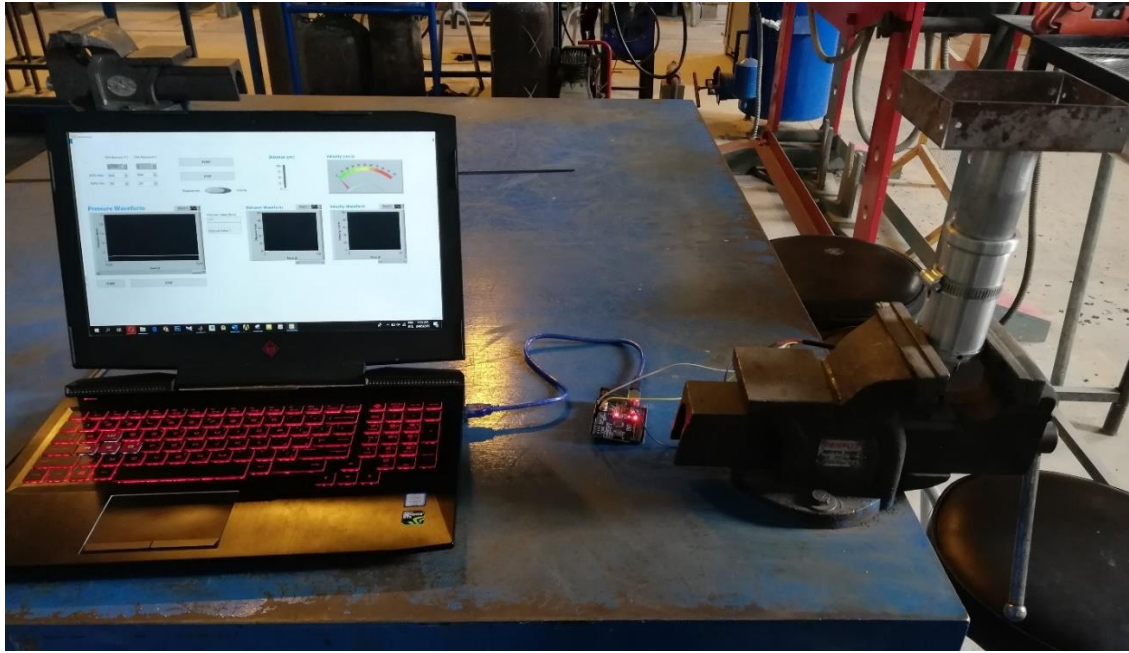


Figure 39: Dynamic Testing

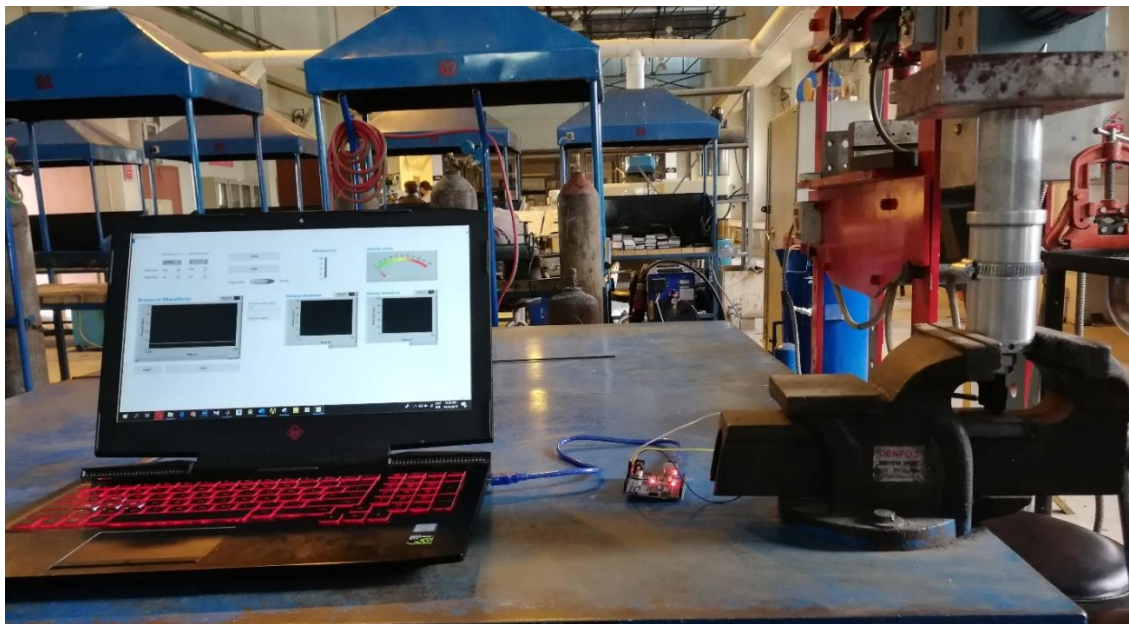


Figure 40: Dynamic Testing

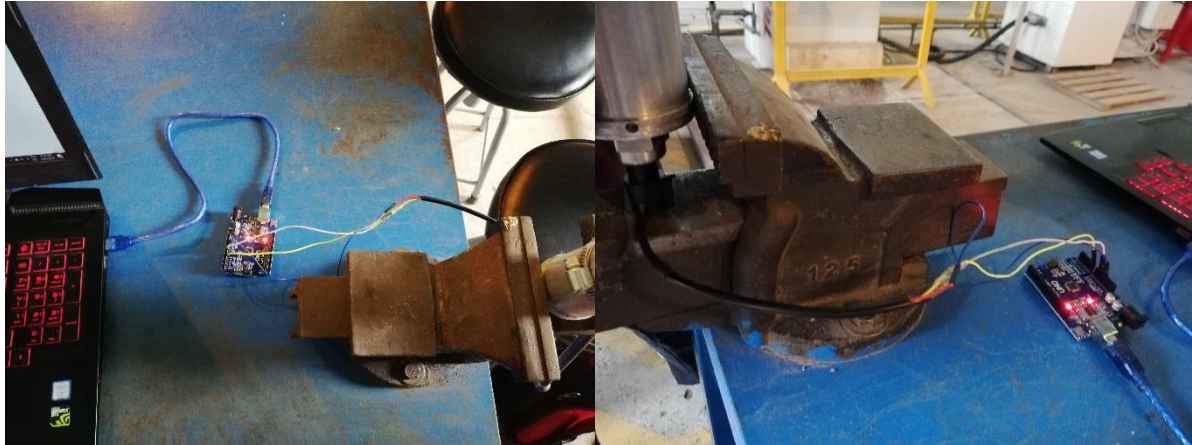


Figure 41: Measuring pressure under load

Table 6: Static Testing Observations and Calculations

Weight (N)	Displacement (cm)	Pressure (kPa)
59.841	2.2	120.7
73.575	2.8	122.1
95.157	3.8	133.3
104.967	4.2	139.7
146.169	4.8	143.6

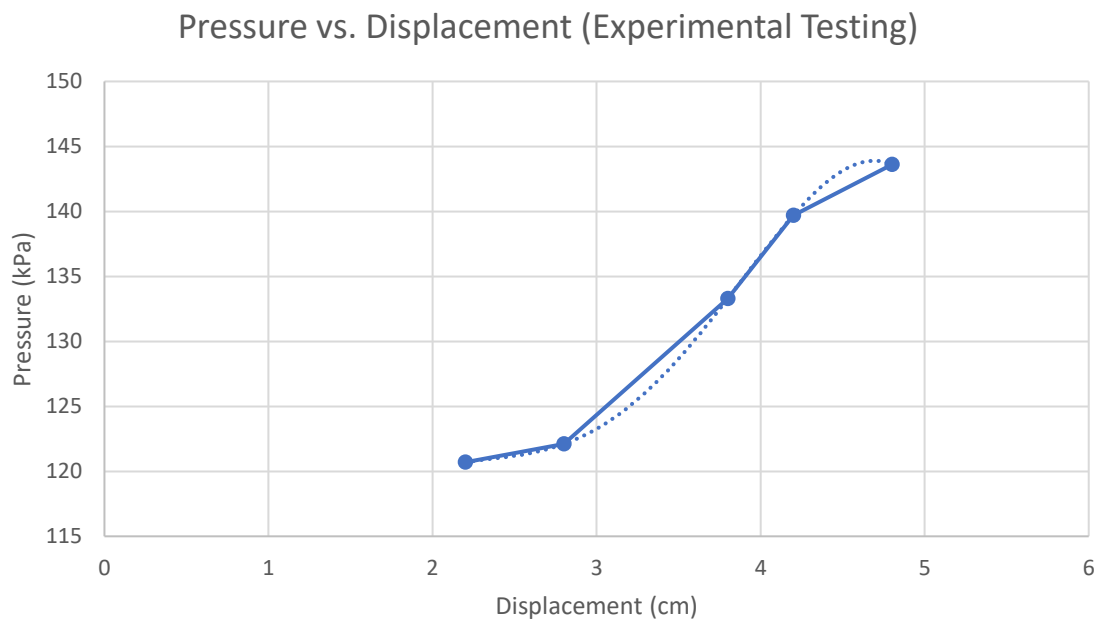


Figure 42: Pressure vs. Displacement (Experimental Testing)

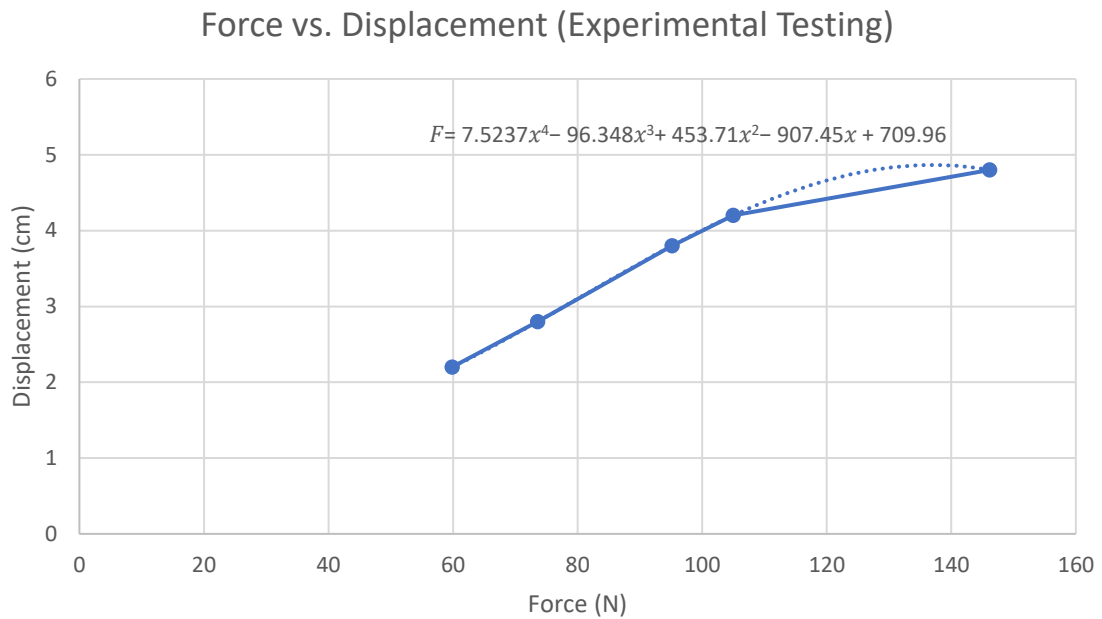


Figure 43: Force vs. Displacement (Experimental Testing)

The relation between the force applied and the displacement produced was obtained by curve fitting as:

$$F = 7.5237x^4 - 96.348x^3 + 453.71x^2 - 907.45x + 709.96$$

By taking derivative of the above equation at known values of x we get the instantaneous values of spring stiffness as:

Table 7: Force vs. Stiffness

Value of F (N)	Value of k (N/m)
59.841	2725.12
73.575	2631.33
95.157	2509.51
104.967	2503.22
146.169	3049.17

Simulink Results for Static Testing:

We started by modeling the strut in SolidWorks. Then we imported the 3D assembly in Simulink and applied prismatic joint between the upper and the lower cylinder. We used the stiffness values gained from experimental testing in the Simulink model and ran the analysis. The Simulink setup is shown below. The joint of interest here is the prismatic joint.

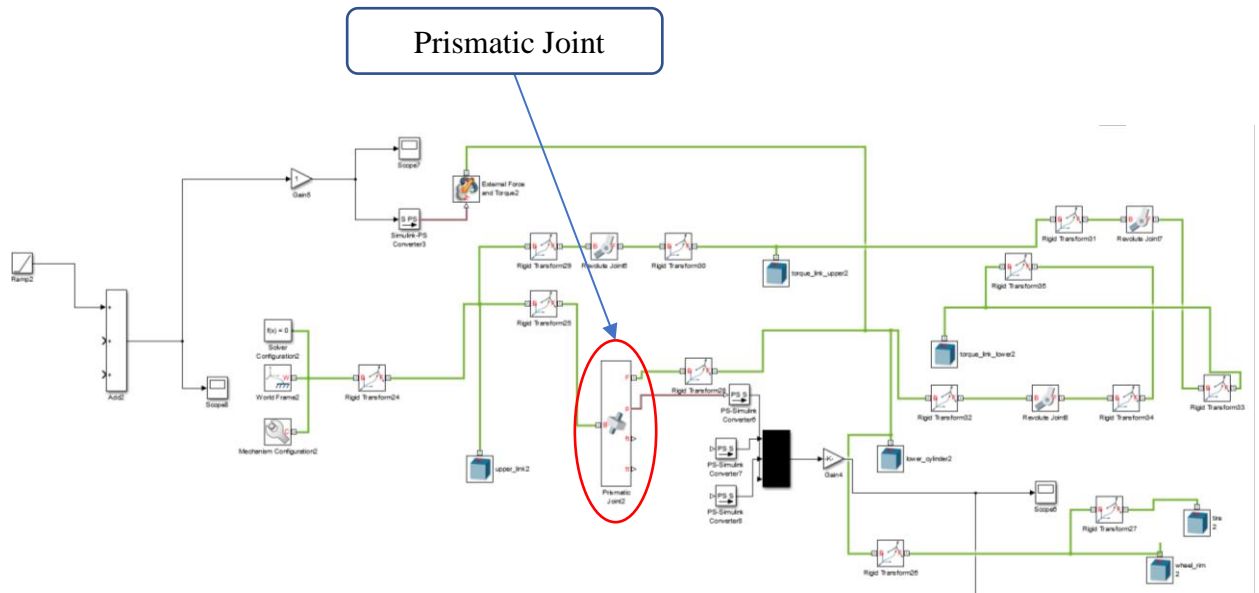


Figure 44: Simulink model

We obtained the displacement vs time curves as shown below:

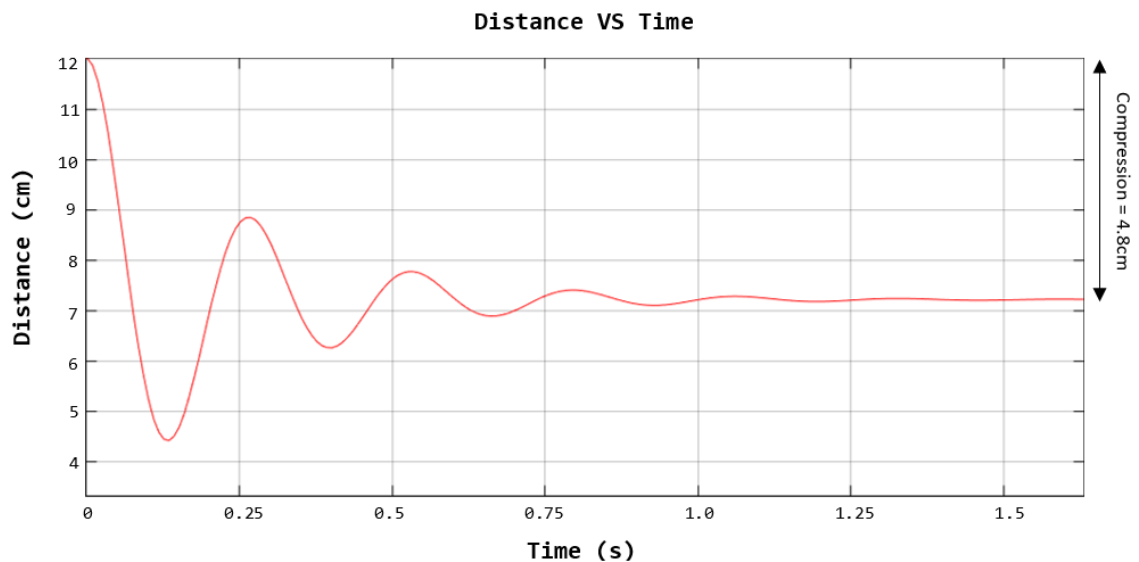


Figure 45: Distance vs. time

We obtained five curves similar to the curve above (for each different value of stiffness) showing the final resting position of the strut. We then compiled the displacement results for different values of the stiffness. The graph we obtained after compiling the Simulink analysis data is as following:

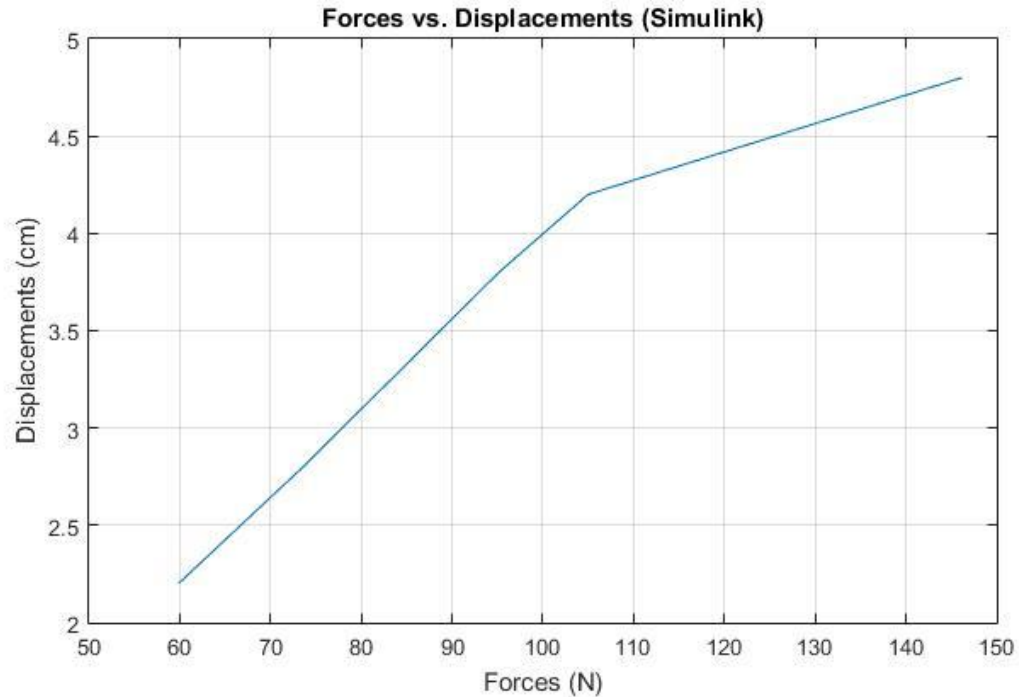


Figure 46: Forces vs. displacements

Comparison:

We observed that the experimental values are very close to the ones obtained from Simulink results. Percentage error was calculated at different points and the maximum percentage error was found to be around 4 percent. Another important observation is that the results verify and validate the stiffness aspect of the strut. This aspect can be completely determined without analyzing the damping properties as the final equilibrium states remains the same irrespective of the damping coefficient as long as the stiffness constant remains the same. The damping coefficient only determines the time after which the disturbance dies down and this aspect cannot be verified during static testing.

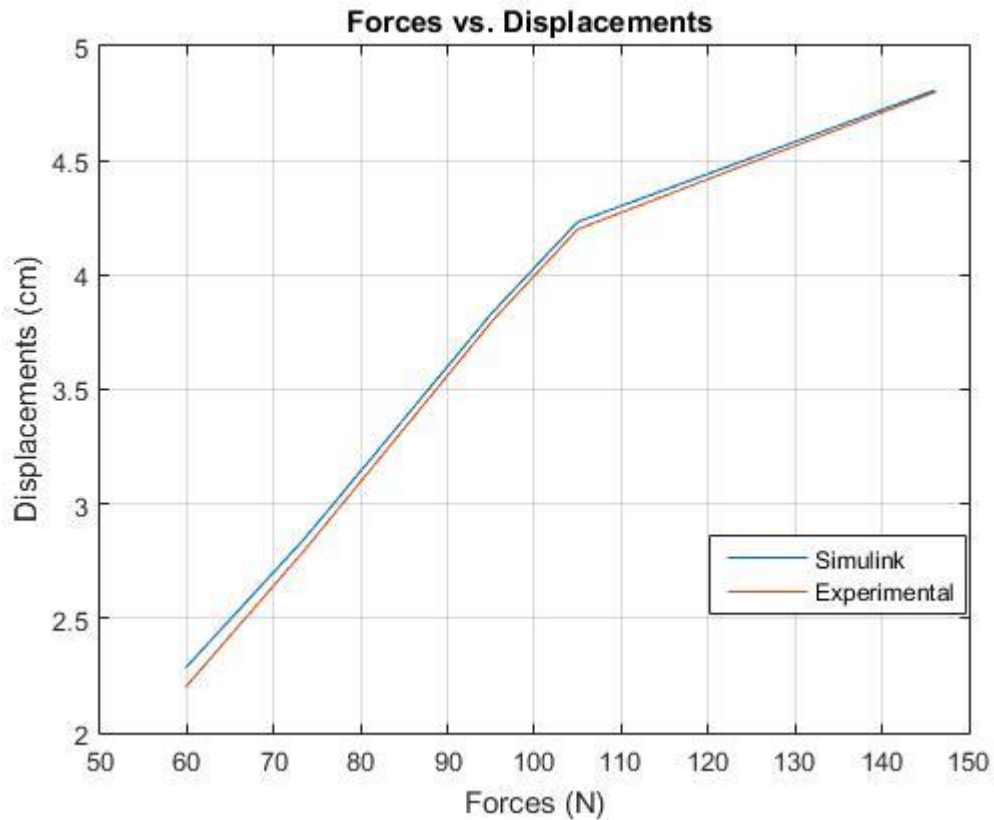


Figure 47: Forces vs. displacements

Dynamic Testing Observations and Calculations:

Initially a height of 1m was chosen and different masses were dropped from this height. The velocity at impact and the total momentum at impact along with the impact force can be calculated as shown below. The time of impact is taken as half a second. The friction in the air has been neglected as the fall distance is only 1 meter and the object does not attain its terminal velocity in such a short distance and the decrease in velocity because of drag is not significant. The values are tabulated below:

The velocity at impact is:

$$V = \sqrt{2gh} = \sqrt{2 \times 9.81 \times 1} = 4.43m/s$$

Table 8: Forces corresponding to Mass

Mass (Kg)	Momentum (Kgm/s)	Force (N)
5	22.16	44.32
6	26.58	53.16
7	31.01	62.02
8	35.44	70.88
9	39.87	79.74

The displacement values were recorded through the ultrasonic sensor. These values as a function of time were displayed on the LabVIEW interface and were logged into an excel file. The plots for each of the above cases are shown below.

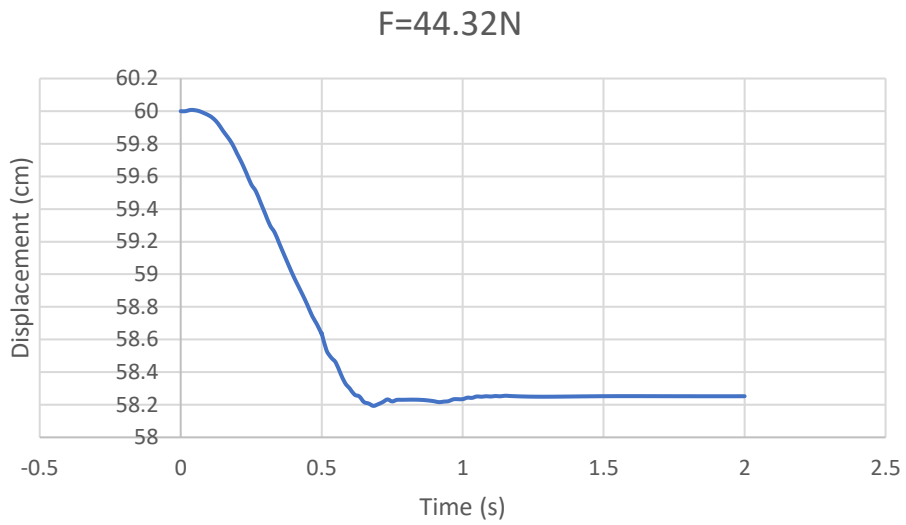


Figure 48: Displacement vs. time ($F=44.32\text{N}$)

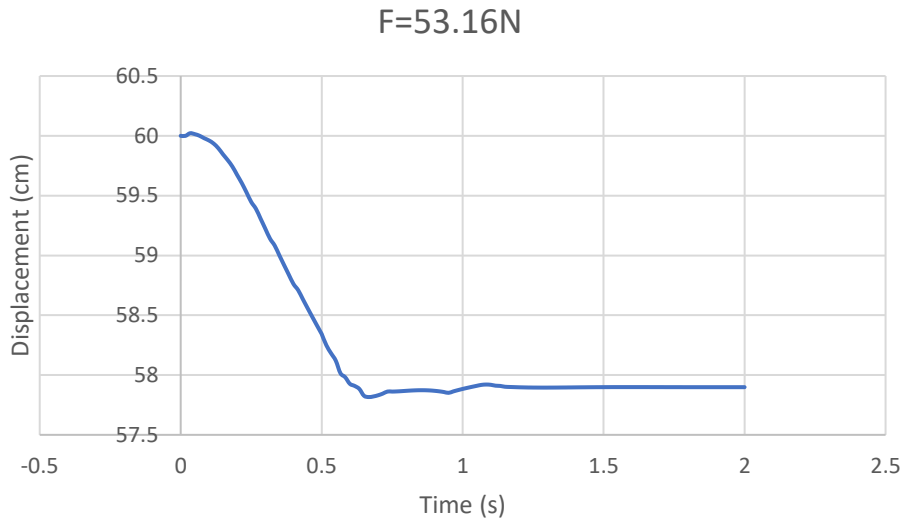


Figure 49: Displacement vs. time ($F=53.16\text{N}$)

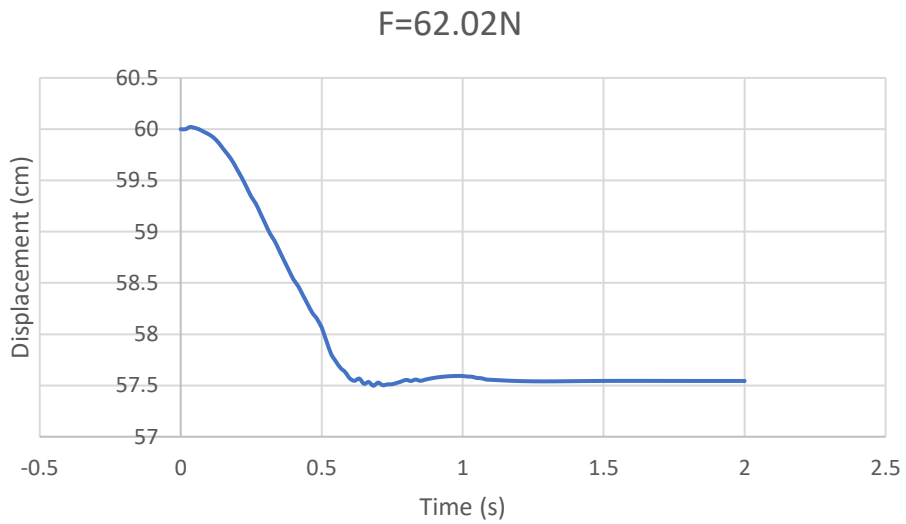


Figure 50 : Displacement vs. time ($F=63.02\text{N}$)

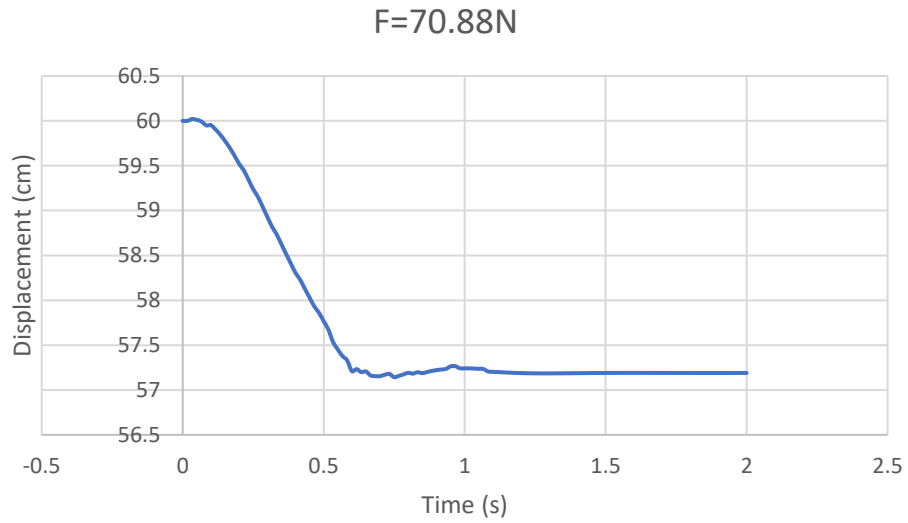


Figure 51: Displacement vs. time ($F=70.88\text{N}$)

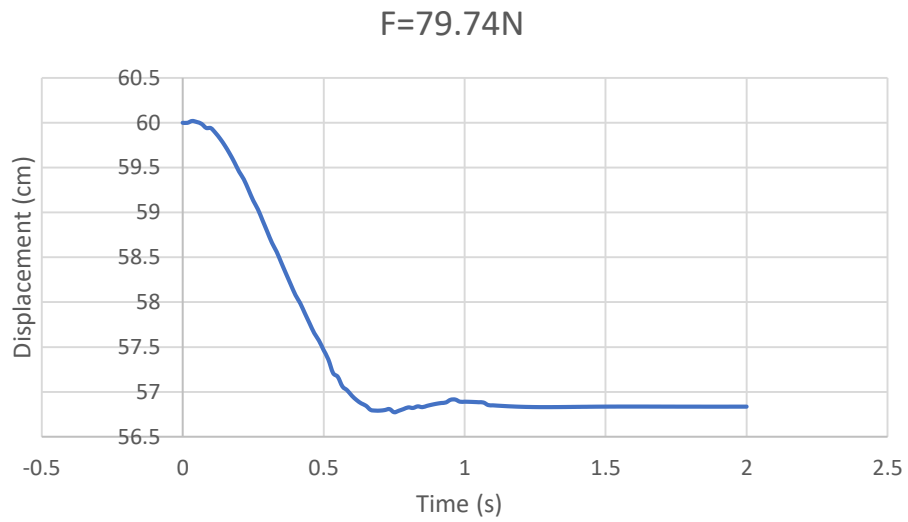


Figure 52: Displacement vs. time ($F=79.74\text{N}$)

Simulink Results for Dynamic Testing:

The forcing function can be estimated to be a linear one because the impact is between two steel surfaces which means force at the start of collision is 0N and steadily and linearly rises to its maximum value by the time the collision ends. These forcing functions were fed to Simulink and the resulting ideal displacement curves are shown below for each of the above-mentioned masses.

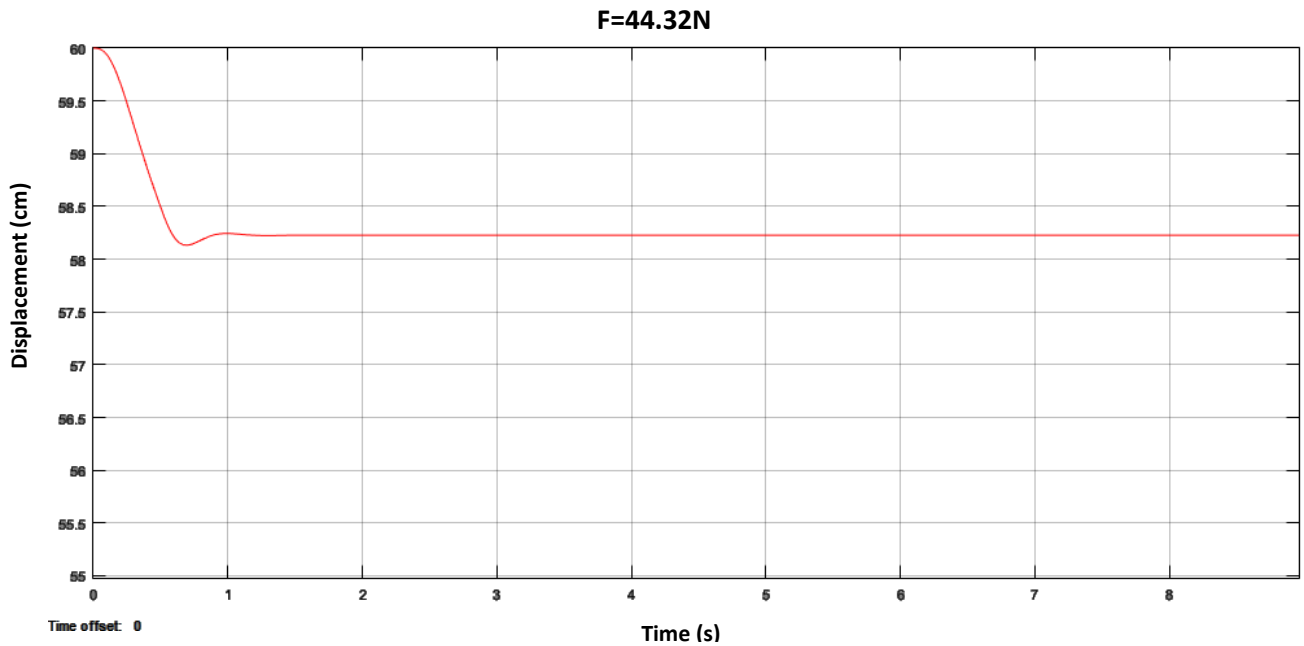


Figure 53: Displacement vs. time (F=44.32N)

F=53.16N

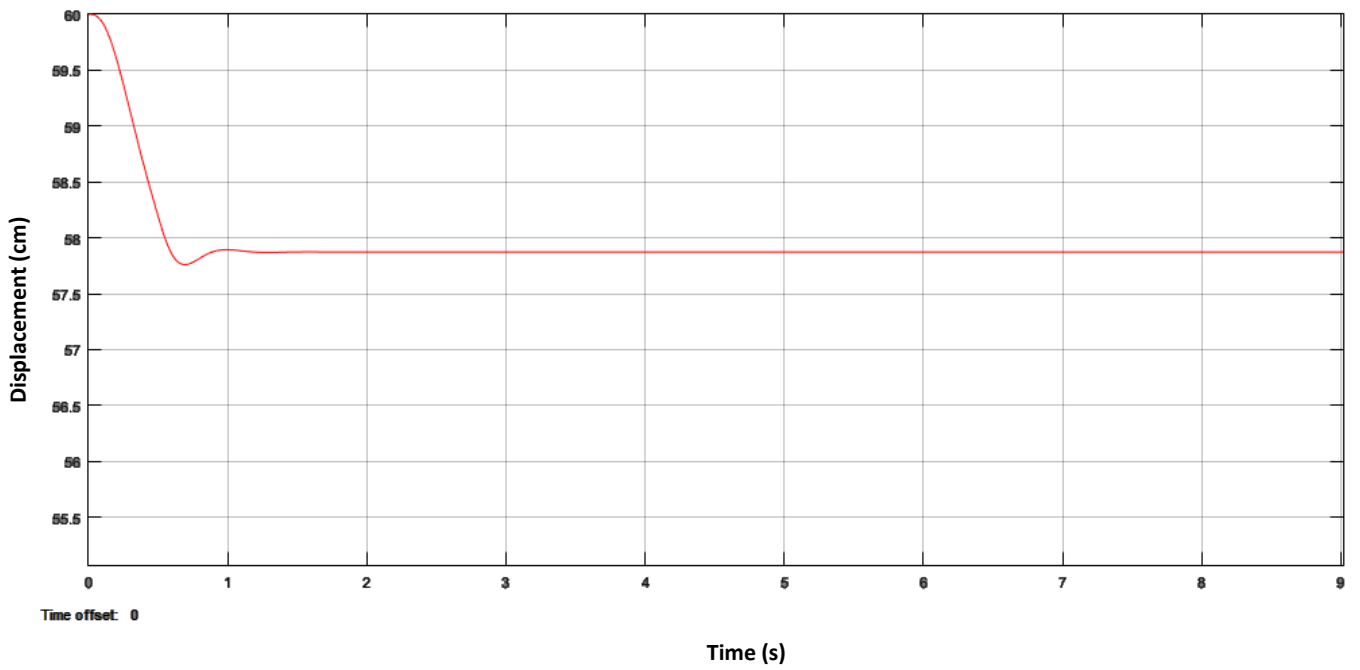


Figure 54: Displacement vs. time

F=62.02N

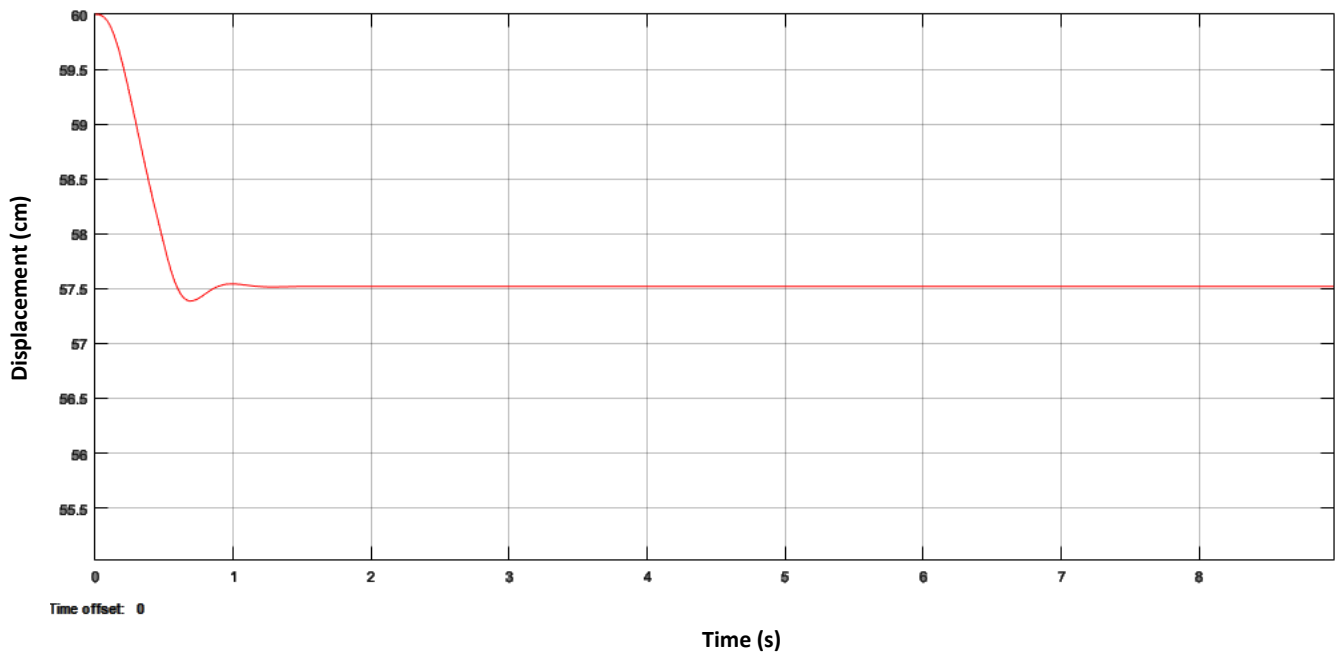


Figure 55: Displacement vs. time

F=70.88N

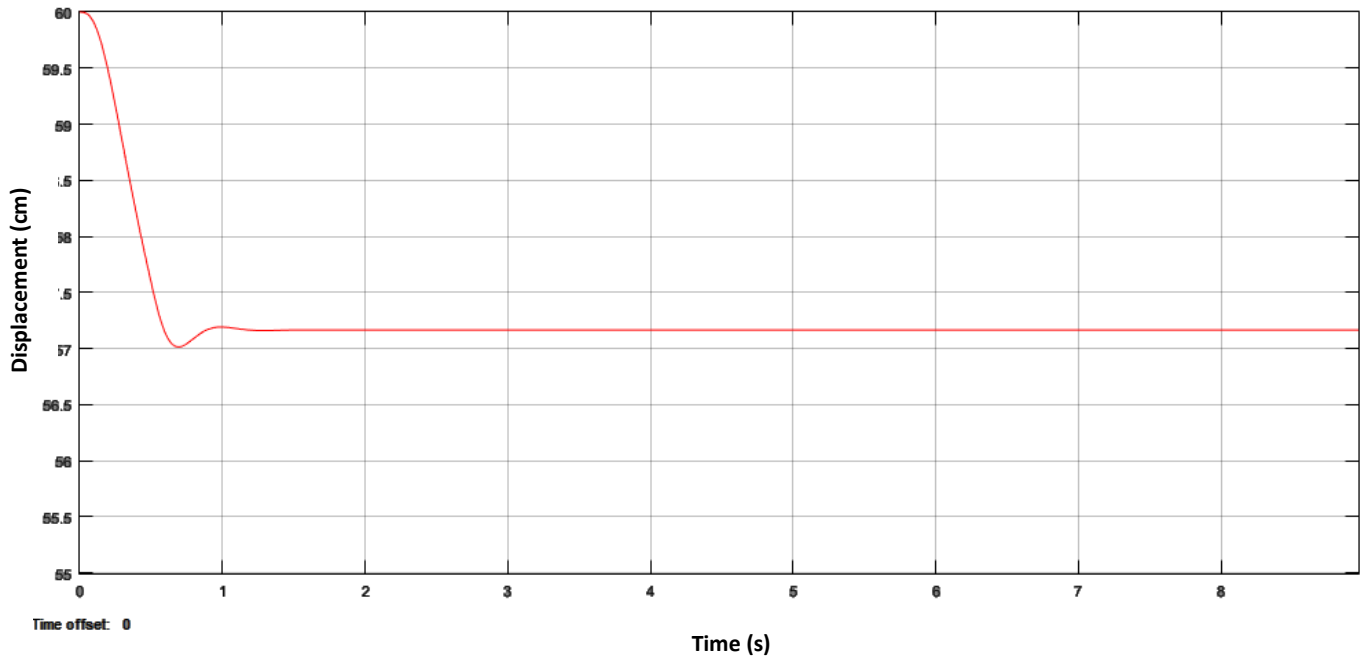


Figure 56: Displacement vs. time

F=79.74N

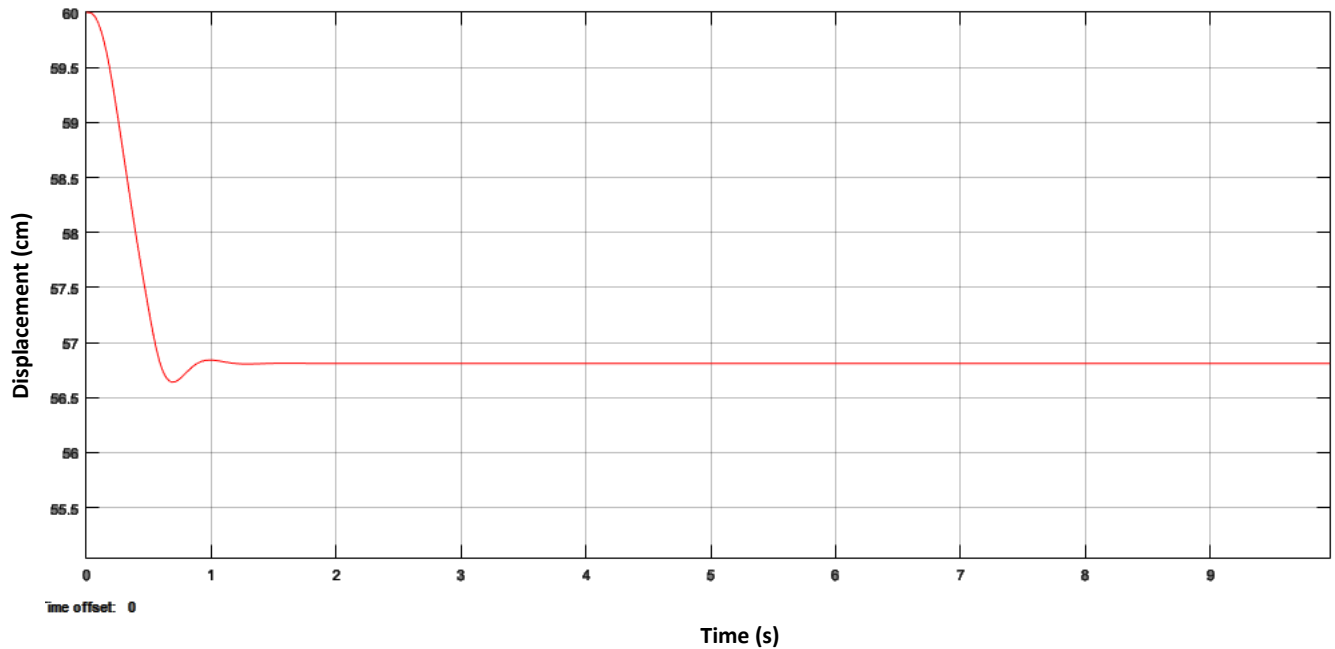


Figure 57: Displacement vs. time

Comparison:

The displacement vs time plots for given applied forces have been plotted on a single graph to see how the experimental values match up with those of the Simulink simulation. We observe that the two curves follow the same pattern however identical values are seldom found. There is some continuous offset or an error which can be attributed to several reasons. Some of which are mentioned below:

- The air drag during the fall of the experimental weight was neglected.
- Losses through fluid and air friction inside the strut were assumed negligible.
- Energy dissipation was assumed uniform.
- The steel surfaces were assumed free of any contaminants thus allowing for a perfect 1D collision.
- Any damping caused by the variation in oil grade or composition from those specified on the manufacturer's tag.
- Any air leakage that might have taken place despite the twin seals.
- Noise in the ultrasonic sensor
- Unwanted vibration in the apparatus

This aspect of testing shows how quickly the vibration damps or dies down in the strut. This behavior is controlled by the damping coefficient of the strut. This is a measure of how fast the energy is dissipated from the spring energy (here the energy of compressed air) to other forms.

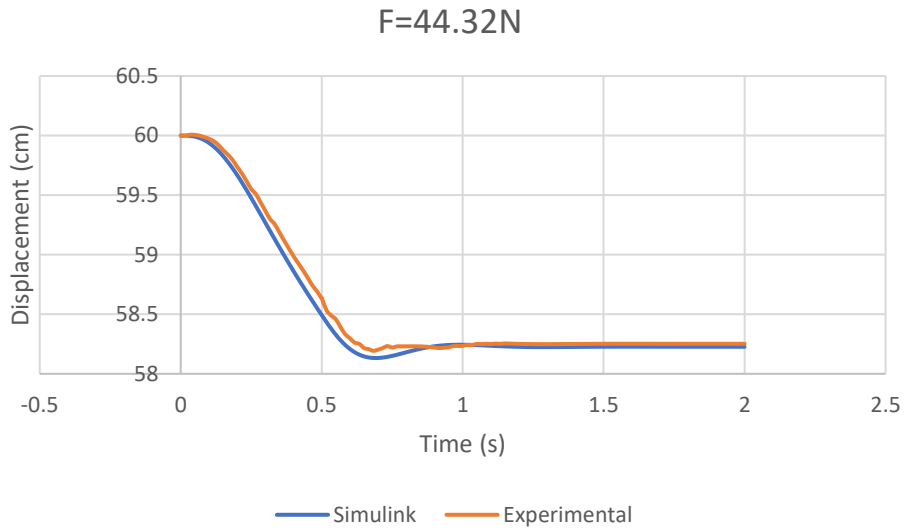


Figure 58: Displacement vs. time ($F=44.32\text{N}$)

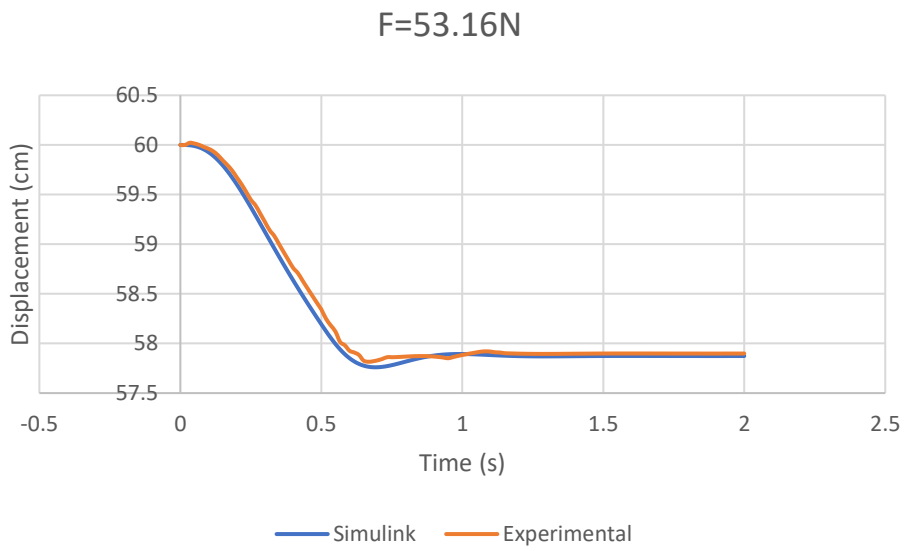


Figure 59: Displacement vs. time ($F=53.16\text{N}$)

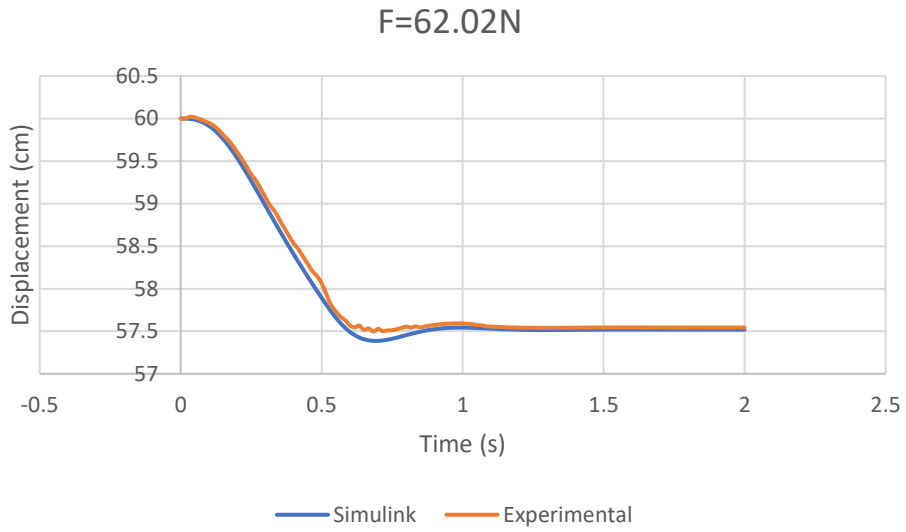


Figure 60: Displacement vs. time ($F=62.02\text{N}$)

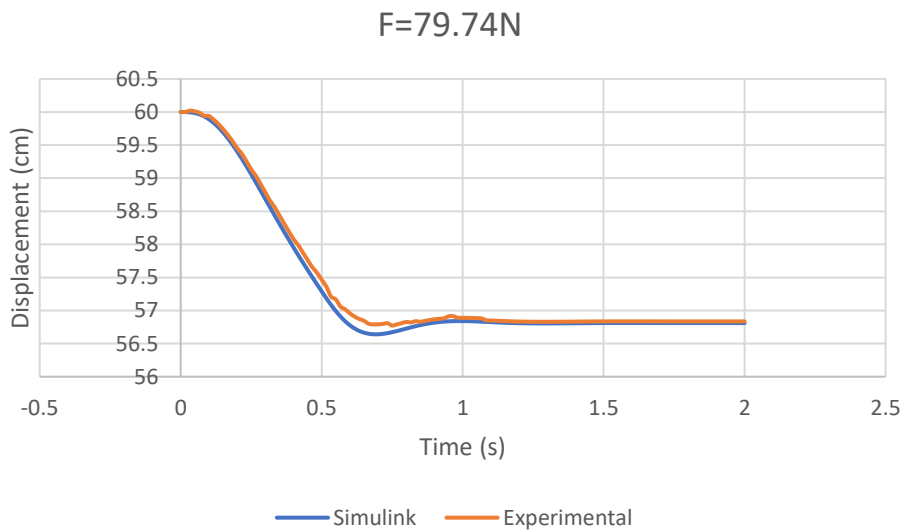


Figure 61 : Displacement vs. time ($F=79.74\text{N}$)

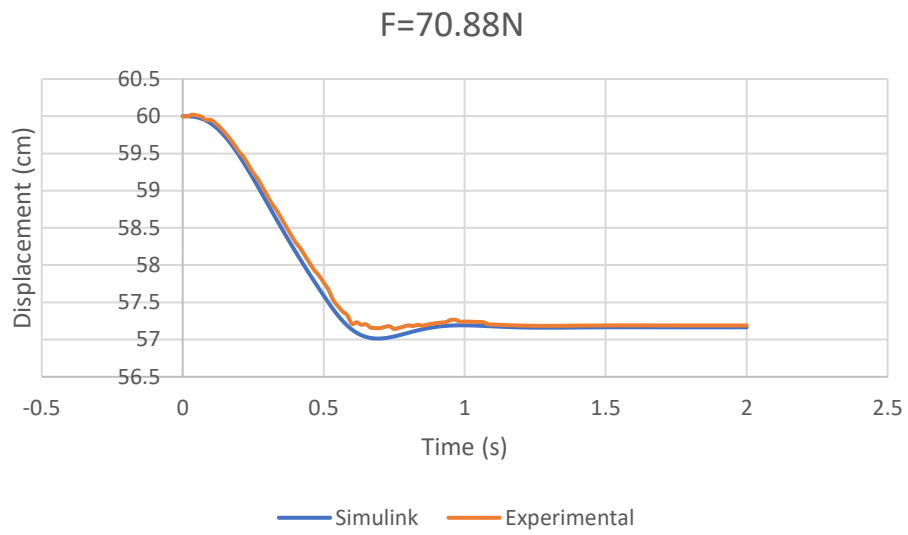


Figure 62 : Displacement vs. time ($F=70.88\text{N}$)

CHAPTER 5: CONCLUSION

The project initiated with a literature review of airplanes, their landing gears, the assemblies, different configurations, roles that different parts play. This review was general and not limited to any particular type of aircraft. Then we moved onto UAVs and their landing gears in particular. We studied Predator MQ1, Predator MQ9 in detail and familiarized ourselves with its landing gear, loads, and other systems accompanying the landing gear system including braking system, steering, extension and retraction. To initiate the design process, we modeled a generic oleo strut from designs we obtained from recent research papers. We combined these parts into an assembly. After the model was ready, we rigged it in ANSYS and conducted static and dynamic analysis. Along with ANSYS we used Simulink to run further analysis the results of which are discussed above.

Similar projects have been done in the past with the general aim to improve the crashworthiness of the landing gear. Such research papers and related work has been referenced in the references. However, we took a different approach. We started studying the design from scratch and after completely defining it mathematically, we tweaked different parameters to best suit our landing gear requirements for a UAV similar to Predator MQ-1.

The static testing helps compare the stiffness constant of compressed air in the strut to the Simulink values. The results were quite accurate with very negligible error. It determines the static or equilibrium position of the strut after a load has been applied.

The dynamic testing helps compare the damping coefficient of the compressed oil and air in the strut to the Simulink values. These results did show some deviation from the original values. However, the trend was identical and the overall error was basically due to not so accurate testing rig. This part of the testing determines how quickly the strut comes to rest after a load has been applied.

Future Aspects:

The future aspects of our work include the possibility of certain modifications to suit it to any other UAV. The general mathematical model comprising of hydraulic model and pneumatic model remains the same, and hence can be excited with different load data set according to the type of UAV. This makes it applicable for general purposes and thus increases its utility. Moreover, further research into the fluid properties (a separate branch of hydraulics) may be undertaken to further enhance the performance of the landing gear. The Simulink model is such that retraction system may also be attached if needed. All the required hydraulic actuators and control blocks are already available in the library and are only a click away.

Thus, our model provides a platform for the expansion of landing gear design. Research into the material properties, compounds, alloys, composites and the treatment used at joints is another avenue which may be undertaken to further the cause of improved crashworthiness of a landing gear. The wheel assembly which was ignored during the project, since a custom model was chosen, may also be modified using topology optimization and using better materials with improved strength and stress bearing

properties. Fatigue analysis, although not strictly related to crashworthiness of a landing gear may also be incorporated into the design phase. Consideration of fatigue failures and applying certain improvements causes increased reliability at times of severe crash landings where impact forces may exceed the maximum expected values.

REFERENCES

- [1] <https://www.boldmethod.com/learn-to-fly/systems/how-the-4-types-of-landing-gear-struts-work/>
- [2] https://en.wikipedia.org/wiki/Oleo_strut
- [3] <https://www.shockwarehouse.com/news/differenceshocksstruts.cfm>
- [4] <https://en.wikipedia.org/wiki/Strut>
- [5] <https://www.monroe.com.au/trade-corner/tech-info/struts/what-struts-do.html>
- [6] <http://howthingsfly.si.edu/ask-an-explainer/what-materials-are-used-make-landing-gear>
- [7] <https://www.quora.com/Which-materials-besides-titanium-are-used-to-make-aircraft-landing-gear-systems>
- [8] https://www.faa.gov/regulations_policies/handbooks_manuals/aircraft/amt_airframe_handbook/media/ama_-_20%20Ch13.pdf
- [9] <https://fiberdynamics.net/uav-landing-gear-strut-resin-transfer-molding.html>
- [10] Improved Design of Lock-lever in an Aircraft Landing Gear Young-Doo Kwon
Department of Mechanical Engineering and IEDT, Kyungpook National University,
Daegu, 702-701, Republic of Korea
- [11] Modal Analysis of Typical Landing Gear Oleo Strut, Dr. N. Srineevasa Babu,
Shinas College of Technology, 2455-1457, India
- [12] Flight Loads of Mini UAV, Rzeszow University of Technology, 35-959
Rzeszow, Poland
- [13] Selection and Analysis of the Landing Gear for Unmanned Aerial Vehicle, Jigar
Parmer, Vishnu Acharya, Dr. Challa, 0976-6340, Maharashtra, India
- [14] Design and Structural Analysis for Weight Optimized Main Landing Gear for
UAV under Impact Loading, Raeen Fida Swati, Dr. Abid Ali Khan, Institute of Space
Technology, Islamabad, Pakistan
- [15] Design and Structural Analysis of Weight Optimized Main Landing Gears for
UAV under Impact Loading, Raees Fida Swati, Dr. Abid Ali Khan
- [16] Landing Gear Layout Design for Unmanned Aerial Vehicle, Akhilesh Jha.
- [17] Aircraft Design - A Conceptual Design by Daniel P. Raymer, Sylmar, California